Delft University of Technology

Modeling embodiment during the rubber hand illusion

A dynamical model validated by a time-varied experiment

Brenda Knijnenburg

TU Delft

Modeling embodiment during the rubber hand illusion

A dynamical model validated by a time-varied experiment

By

Brenda Knijnenburg

In partial fulfillment of the requirements for the degree of

Master of science
in BioMedical Engineering

at the Delft University of Technology,
to be defended publicly on Monday October 31, 2022 at 14.30 PM.

Supervisors:	Dr. Ir. Arkady Zgonnikov,	Cognitive Robotics, TU Delft
	Prof. Dr.-Ing. habil. Philipp Beckerle,	Mechatronics, FAU Erlangen-Nuremberg University
Thesis committee:	Prof. Dr. Ir. Martijn Wisse	Cognitive Robotics, TU Delft
	Dr. Ir. Gerwin Smit	BioMedical Engineering, TU Delft

An electronic version of this thesis is available here

TU Delft

Preface

This master's thesis is the final research for my master's in BioMedical Engineering and is developed at the Cognitive Robotics department at the TU Delft. During my master's at the TU Delft and my bachelor's at the TU Eindhoven, I learned much theory needed to finish this thesis. During my bachelor, I already learned a lot of the practical knowledge required to carry out research. This research was always done in groups. During my thesis, I got challenged to do this on my own and on a more significant human subject project. I became more familiar with the subject step by step, and even today, I seem to learn more about the fascinating illusion of the rubber hand. Along the process, I got more and more enthusiastic about my research. Therefore, I am proud to present the experiment results and the from-scratch-created dynamical model.

My research aimed to create a dynamic model related to the embodiment of the rubber hand illusion. This has been done by integrating empirical findings from the literature into a model. Besides, results from a self-conducted human subject experiment have been used to further validate and improve the model. By doing both a human subject experiment and creating a dynamic model, I was forced to come out of my comfort zone and learn more about being an engineer, myself, and the things I can do.

The presented work would not have been made possible without the help of my supervisors: Arkady Zgonnikov and Phillip Beckerle. I would like to thank them for their help and critical thinking throughout the process. Especially Arkady Zgonnikov for the efficient weekly meetings and his support in my decisions during the project. I also would like to thank my parents and brother for helping me wherever they could and being there for me whenever I needed them. Finally, I would like to thank my friends and housemates for their support during the mental ups and downs that are part of doing a master's project. Besides that, I would like to thank them for the conversations we had about the project, which kept me critical of my own work and gave me the motivation to keep up the good work.

Brenda Knijnenburg
Delft, October 2022

Contents

Abstract

A common method to investigate multisensory integration is using multisensory illusions. The rubber hand illusion is one of the best-known multisensory illusion used in clinical applications. By stroking a visible rubber hand and the participant's occluded hand, the illusion arises that the rubber hand belongs to the participant. Possible applications based on this illusion are for neurorehabilitation or developing robotic devices. These applications are still in a very initial state, and this thesis aims to take these possible applications a step further. The thesis provides the results of a rubber hand illusion experiment over time and a dynamic model related to the embodiment of the rubber hand. The dynamical model can visualize the proprioceptive drift that arises from the illusion and predict the time it takes to experience it. The results of the experiment and other empirical findings from the literature form the basis of the model. The experiment measured these factors and the feeling of ownership and agency over time. The results from this experiment have much variance but are in line with the literature. The dynamical model fails to visualize the body ownership and agency results. Adding extensions and improvements could make this dynamic model more complete and applicable in many research fields.

1 Introduction

The rubber hand illusion is a phenomenon involving cross-modal, and multi-modal integration [1]. Cognitive neuroscience studies use it to describe the influence of visual and somatosensory cues on body representations [1]. The rubber hand illusion is not only of interest in the cognitive neuroscience department but has also extended into other disciplines. The rubber hand illusion has been used in philosophy to explain the concept of body ownership and what exactly contributes to one's 'self', as well as in psychology for the existence of dis-sociable body representations [2]. Botvinick and Cohen [3] propose that the feeling of ownership in the rubber hand illusion is mediated by integrating multiple senses. Suggesting that ownership is related to a match between the visual, tactile, and proprioceptive signals and the individual's internal representation of the hand [1].

Botvinick and Cohen [3] were the first to describe the rubber hand illusion. In their study, the seen stroking of the rubber hand while synchronously feeling the stroking of one's hidden hand was enough to conduct a feeling of ownership over the rubber hand in most participants. Besides the feeling of ownership, they observed distortion in the proprioceptive information. The researchers asked the participants to close their eyes after the stroking and indicate with their non-stimulated hand the location where they perceived their hand. The perceived location was closer to the rubber hand. This proprioceptive drift varied per participant and duration of the stroking.

Many studies on rubber hand illusions have been published since the original study of Botvinick and Cohen [3]. These studies use different methods for quantifying the effects of the illusion [4]. For example, the skin temperature [5] and histamine reactivity [6] have been measured. A more interesting quantifying method is measuring the time it takes to perceive the illusion. This onset time, as well as the proprioceptive drift and body ownership, could be important for scientists who want to apply these principles into other fields such as neurosurgical treatment [1], neuro-rehabilitative therapies [7], advanced prosthetic research [1, 7] or understanding different pathologies [1, 7].

To apply the principles of the rubber hand illusion in these fields, more should be known first. Understanding the relationship between the onset time, proprioceptive drift, and ownership and the process over time is necessary. Furthermore, a patient-specific model is needed for applicability rather than an assumption based on the results of a population. Existing models of RHI are not dynamic and therefore do not describe important measures such as the onset time, the proprioceptive drift, and the body ownership. Previous research has tried to model the multisensory illusion computationally. These models use the Bayes rule [8] to solve the conflict between the visual, proprioceptive, and tactile stimuli. Two different approaches can be found in literature, the bottom-up model [9] and the top-down model [10].

The bottom-up model [9] adopts the Bayesian causal inference model [11] to model the rubber hand illusion. The bottom-up model assumes that the rubber hand illusion only operates on the temporal and spatial information and the cross-model recalibration of these senses. Temporal aspects give information over time; thus, the stroking and the spatial aspects are related to the distances between the hands. The illusion creates a conflict between the spatiotemporal senses, which it tries to minimize using the mean squared error between the estimates. This type of modeling is called model averaging [12]. Their model can recreate the results from the experiment; A delay between the visual and tactile stroking will not create the illusion, while synchronous stroking does. Additionally, increasing the distance between the hand will weaken the illusion. A drawback of their model is that it cannot visualize the differences between individuals and the change over time.

The top-down model [10] considers individual differences by introducing higher-level representations of the body. These body representations are related to the body's visual, anatomical, and structural properties. According to their model, body ownership during the illusion arises as an interaction between multisensory input and modulations exerted by stored and online internal models of the body. Their model explains the comparisons made during the illusion rather than a computational model. It also fails to give a dynamic model in which the internal models change over time.

None of these models present the ability to model the dynamics of the illusion. They fail to visualize the body ownership and the proprioceptive drift over time. They further fail to visualize the expected time it takes for the illusion to occur. This thesis aims to address these limitations by modeling the dynamics of the body ownership, the proprioceptive drift, and the onset time during the rubber hand illusion. Since the mechanism underlying the illusion is the multisensory conflict between different senses and a conflict between the internal model and the external signals, the proposed dynamical model combines ideas of existing bottom-up [9], and top-down [10] models. However, since both these models do not describe the change over time, the need for another algorithm arises. The proposed model addresses this by utilizing Kalman filtering. The Kalman filter

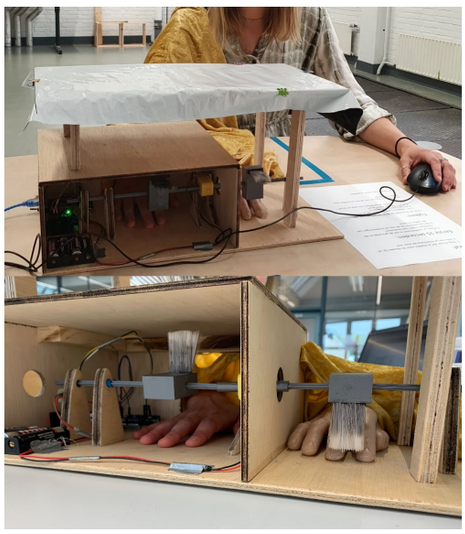

Figure 1: Experiment set up inspired by Sivasubramaniam et al. [14], and updated to meet the experiments requirements.

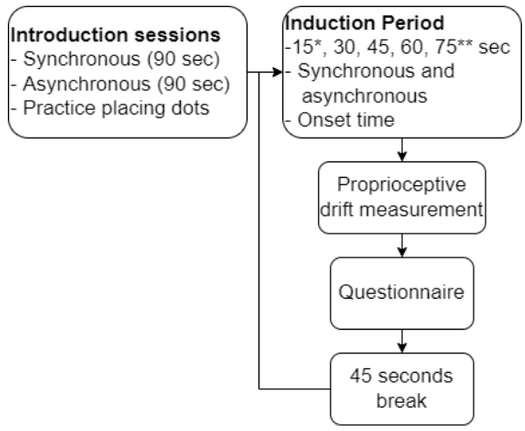

Figure 2: Overview of the experimental design. * ten participants received an induction time of 15, 30, 45, and 60 seconds. ** for the other participants, the 15-second induction was replaced with 75 seconds.

provides estimates of an unknown variable given the measurements observed over time [13].

In addition to the model, this thesis reports an original experiment with human participants designed and executed to investigate the dynamics of the illusion. It was hypothesized that over time the proprioceptive drift shifts more to the rubber hand and that the ownership statements are rated higher with a longer induction time [15] and that the illusion was more likely to arise in the synchronous condition [16]. Finally, I analyzed the model's validity based on the experiment's results.

Section 2 provides the experimental setup and protocol as well as the results of the experiment. More information about the proposed dynamical model is found in Section 3.

2 Experiment

The experiment's main objective is to investigate the dynamics of the illusion and the relationship between the onset time, the proprioceptive drift, and the body ownership.

2.1 Materials and methods

2.1.1 Participants

A total of 37 participants (14 male, 23 female), between 19 and 29 years old (with a mean age of 24 years) and a hand size between 15 and 21 cm (average of 17.6 cm) gave written consent to participate in the study, which had the Human Research Ethics committee of the TU Delft's approval. For all participants, it was the first time they experienced the illusion. A compensation of €10 was given for their participation.

2.1.2 Materials

I used an automated setup for the induction of the illusion. Figure 1 shows a visualization of the setup, which is similar to Sivasubramaniam et al. [14]. The stimulation device comprises three significant components: the mechanical brushing mechanism, the electronic control system, and the peripherals. The brushing mechanism and control system are housed inside a wooden box.

The brushing mechanism is attached to the mechanical components and fixated to a stage. Two slots secure the brushes fastened to the horizontal rotating shaft, allowing for synchronous and asynchronous stimulation [14]. The distance between the two brushes is initially fixed at 15.7 cm. Wooden shaft holders hold the rotating shaft in place and minimize shaft bending and pitching.

An addition to the setup makes measuring the proprioceptive drift possible. This addition consists of a wooden plate with four legs supporting the plate (Figure 1). A white erasable foil with paper clips is fixed on this plate during every measurement. Designs and codes for this setup are available in the supplementary data.

A white noise track (mono track, 44,100 Hz sampling frequency with 32-bit float) was generated using Audacity software (Version 2.2.2) with an amplitude of 0.05 and exported to a .wav file [14]. The rubber right hand used in the experiment is a prosthetic glove from Fillauer with item description: 130910Y021. A cloth covers the participants' right arms during the experiment. The provided code from Sivasubramaniam et al. [14] was updated to meet the experiment's needs.

2.1.3 General procedure

Before the experiment, the participants removed all jewelry from their hands to keep the visual congruence with the rubber hand as high as possible. The participants were seated comfortably at a chair behind a desk on which the experimental setup was placed. The participants placed their right arm inside the wooden box and positioned their body midline in front of a blue line. This blue line was placed so that the setup was placed 30 cm in front and 10 cm lateral of the participant. Therefore, the total distance between the body midline and the middle finger of the rubber hand was approximately 23 cm.

A within-subject design was used in which all participants first experienced two introduction sessions, after which the experiment began. This session consisted of 90 seconds of synchronous stroking followed by 90 seconds of asynchronous stroking (500 ms delay). Then there was a practice of identifying the location of the own hand by placing the dots on the foil. This practice session is used as the initial guessed location of the own hand.

The experiment consisted of four stroking conditions, either synchronous or asynchronous, resulting in eight conditions. The first 10 participants received an induction duration of 15, 30, 45, and 60 seconds of stroking. For the remaining 27 participants, the researcher replaced the 15-second stroking with an induction time of 75 seconds. The order of conditions was pseudo-randomized, and after each session, there was a resting period of 45 seconds. The entire experiment took approximately 1 hour.

During each condition, the participants indicated the moment they felt the rubber hand was their own if they felt it. After the induction period, the participants indicated where they felt their hand and filled in an embodiment questionnaire. (Figure 2)

2.1.4 Onset time

I wrote a Python code to measure the time it takes for participants to experience the illusion. The participants received a mouse and clicked on the right mouse button as soon as they experienced the illusion with their left hand. After this button press, the experiment continued till the end of the stroking. Lane et al. [17], and Zopf et al. [18] used this type of measurement as well. Instructions were placed on the table to remind the participants when to press the button.

2.1.5 Proprioceptive drift

After the stimulation period, the participants closed their eyes and placed dots on the fixated erasable foil on top of a wooden plate (see Figure 1). They placed the dot with a marker on the location where they felt their hand. After placing a dot, they had to stretch their left arm again to receive another colored marker. Once three dots were placed on the foil, the researcher replaced it with another foil, and the participants could open their eyes again.

2.1.6 Questionnaire

An embodiment questionnaire measured the subjective strength of the illusion. This questionnaire is similar to the one used by Riemer et al. [19]. The questionnaire consists of 6 statements stated in the enumeration below. Answers are given in a 7 point Likert scale, ranging from -3 (*strongly disagree*) to 3 (*strongly agree*). Questions 1&2 are related to ownership, 3&4 to agency, and questions 5&6 are control statements. The questions were randomized during each session.

Questionnaire:

1. It felt as if the rubber hand was my own hand
2. It seemed like the rubber hand was part of my body
3. It seemed like I could grab something with the rubber hand
4. It seemed like I could make a fist with the rubber hand
5. I had the sensation that my hand was numb
6. It seemed like my hand had disappeared

2.2 Results

The analysis includes the results of all participants. The group that received an induction time of 15 seconds does not significantly differ from the group that received an induction time of 75 seconds. Appendix A elaborates the statistics used for the analysis. Here, the statistics compare the outputs against the groups (15 or 75 seconds), the condition they received (synchronous or asynchronous), and the duration of the stroking. I used the Fit linear regression model (fitlm) as the analysis method. Overall the R^2 is small, indicating that the results are noisy and unpredictable.

2.2.1 Onset times

Of the 37 participants, 25 pressed the onset button during the experiment. 13 pressed the button in both conditions, 11 pressed it only in the synchronous condition, and one only in the asynchronous condition. The button was pressed 68 times (n = 24) in the synchronous condition and 24 times (n = 14) in the asynchronous condition. (Figure 3)

The average onset time for the synchronous condition was 21.1 seconds, while the average onset time for asynchronous stroking was 24.3 seconds. There is no significant difference between synchronous and asynchronous stroking ($p = 0.45$). The duration of the experiment and the onset time ($p < 0.05$) show a significant difference. The model itself is not significant ($p = 0.137$).

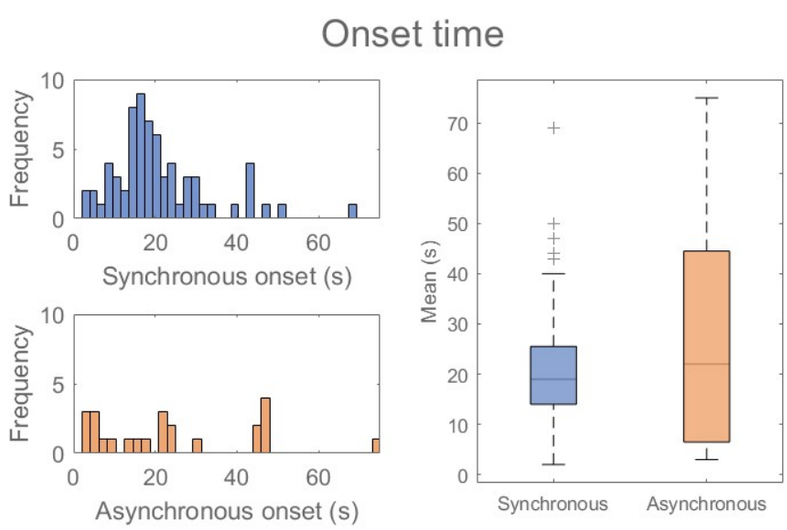

Figure 3: Frequency distribution of the onset times in the synchronous (left-top) and asynchronous (left-bottom) conditions. on the right: Box plots of the onset times in the synchronous (n = 68) and asynchronous (n = 24) conditions.

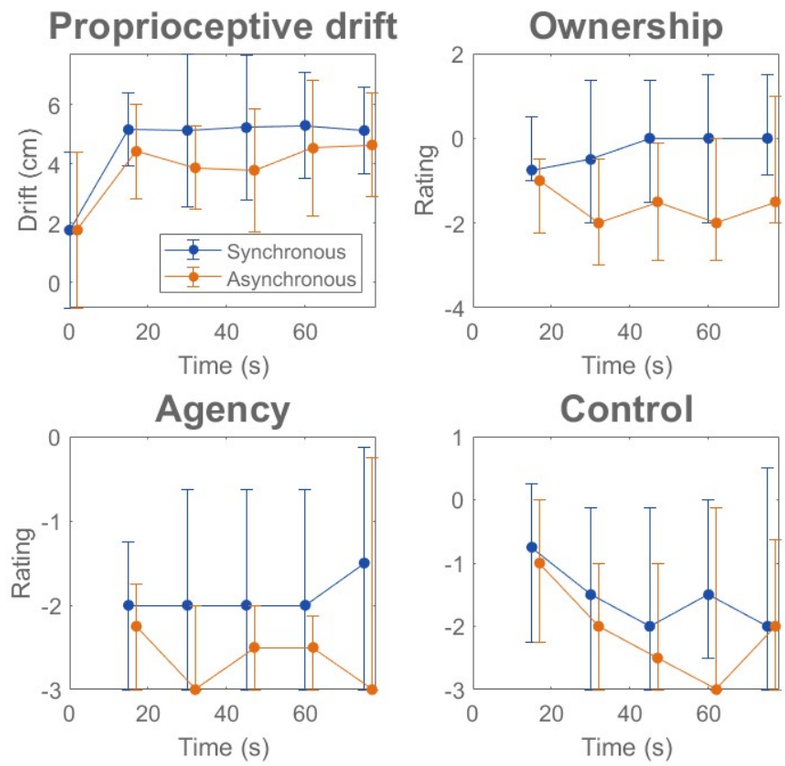

Figure 4: Visualization of the proprioceptive drift and the questionnaire results.

2.2.2 Proprioceptive drift

The proprioceptive drift does not start at zero in this experiment. An initial mismatch between the hand and the perceived location was $1.77 \pm 2.62cm$. After an induction time of 15 seconds, this mismatch increased to $5.16 \pm 1.23cm$ in the synchronous condition and $4.43 \pm 1.59cm$ in the asynchronous condition after 30 seconds (Figure 4 left top). With a longer induction period, this drift stayed approximately the same. The mean of the proprioceptive drift is is significant over time ($p < 0.05$), but not per condition ($p = 0.08$). The model itself is also significant ($p < 0.05$). The average variance of the placed dots on the foils shows no significant linear difference in all tests.

2.2.3 Questionnaire

Then the results from the questionnaire (see Figure 4) are analyzed for the averaged ownership, agency, and control questions. The average of the two statements in each category creates a more solidified subjective output. The data for two participants were lost, and that of another participant for the asynchronous condition at 30 seconds.

Overall it can be seen that the ownership ratings are rated higher than the agency and control questions. For the ownership ratings, the synchronous and asynchronous conditions differ significantly ($p < 0.05$), but the time does not significantly differ ($p = 0.06$). Overall the ownership statements are significant ($p < 0.05$) and have the highest R^2 of all tests with a value of 0.11. The agency statements differ between the synchronous and asynchronous conditions ($p < 0.05$), and the model itself is also significant. This significance is the same for the control statements.

2.2.4 Correlation between onset time, proprioceptive drift and ownership

Finally, the correlation coefficient and the corresponding p-values between the different measurement outputs were calculated for the synchronous (Table 1) and asynchronous condition (Table 2). Appendix B.1 provides scatter plots of these comparisons. Measurements of the onset time are during the induction time, and the proprioceptive drift and ownership measurements are afterward.

For the synchronous condition, all correlation coefficients are significant. The onset time and proprioceptive drift correlate negatively. The correlation between the onset time and the ownership is negative as well. The relationship between proprioceptive drift and ownership is positively correlated. The correlation coefficients in the asynchronous condition are similarly related but show no significance.

Table 1: Correlation coefficients - synchronous. Significance is indicates as: $*p < 0.05, **p < 0.01, ***p < 0.001$

	Onset time	proprioceptive drift	Ownership
Onset time	1	-0.45***	-0.34**
proprioceptive drift		1	0.40***
Ownership			1

Table 2: Correlation coefficients - asynchronous. Significance is indicates as: $*p < 0.05, **p < 0.01, ***p < 0.001$

	Onset time	proprioceptive drift	Ownership
Onset time	1	-0.04	-0.22
proprioceptive drift		1	0.33
Ownership			1

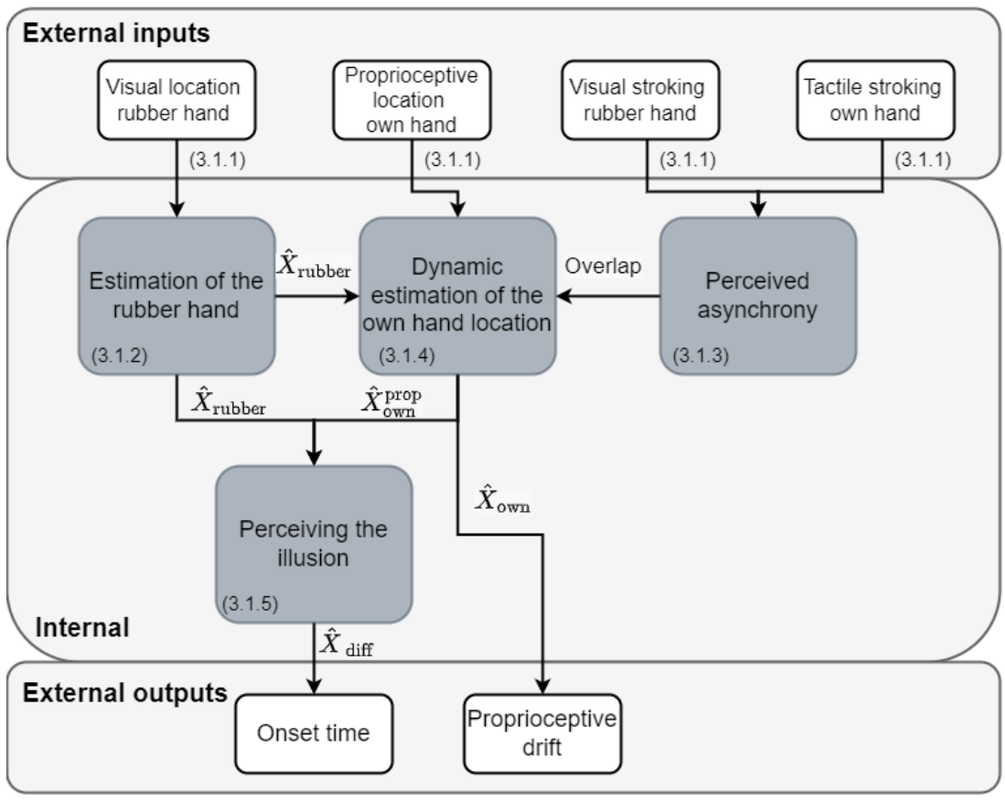

Figure 5: Simplified version of the dynamic model and the relationship between the sections

Table 3: Relation of the used components in the dynamics with the rubber and own hand in the illusion.

	Rubber hand	Own hand
$X^{\text{vis}}_{\text{rubber}}$	✓	
$\hat{X}_{\text{rubber}}$	✓	
$\hat{X}^{\text{vis}}_{\text{rubber}}$	✓	
Pre - existing model	✓	
$X^{\text{prop}}_{\text{own}}$		✓
$\hat{X}_{\text{own}}$		✓
$\hat{X}^{\text{prop}}_{\text{own}}$		✓
$\hat{X}_{\text{diff}}$	✓	✓
$\tau^{\text{vis}}_{\text{rubber}}$	✓	
$\tau^{\text{tact}}_{\text{own}}$		✓
σ_{T}	✓	✓
Overlap	✓	✓

3 Dynamical model

3.1 Method

The Bayesian-based dynamical model proposed here operates on the spatial (the own and rubber hands location), the temporal (the seen and felt stroking), and internal information to estimate the proprioceptive drift and the onset time during the illusion. The dynamic model proposed here will resolve conflicts between internal and external signals as proposed by Tsakiris [10]. Additionally, conflicts between the different cues will be solved, similar to the top-down model [9] with the Bayes rule. The dynamical model is analogous to predictive coding, which is a unified model explaining the interactions in the brain [20]. This theory sees the brain as a hierarchical and bidirectional model. In this hierarchical model, top-down information tries to predict the sensory data coming from bottom-up.

In the proposed model, the Kalman filter constantly updates the top-down information. The Kalman filter consists of two steps, the prediction step and the update step [13]. In the proposed model, the prediction step functions at a higher level in the hierarchy than the update step and works bi-directionally. Due to the combination of the top-down, bottom-up, and Kalman filter, the proposed dynamical model of the illusion can account for the majority of the empirical findings of the illusion. It can also be adjusted to justify individual differences. The figure in Appendix B.2 visualizes the total model diagram, while Figure 5 is a simplified version. Each section has its elaborated diagram for clarification. Table 3 provides an overview of how the used components relate to the own and rubber hand in the illusion.

3.1.1 Representing sensory information

Explanation *The external signals used in the illusion are internally represented as Gaussian distributions.*

The first step in this model is to represent the external signals as internal sensory information. This internal sensory information related to the seen and perceived location of the rubber and own hand and the timing of the seen and felt stroking all have a variance. What precisely the variance of the internal sensory information is, is unknown. The internal sensory information represents the external signals as a Gaussian distribution related to the sensory process [21]. During the illusion, these external signals do not change over time. The variance of the different sensory cues are different [22] and vary per individual [23].

Implementation into the model Four external sensory cues represent the external signals needed for the illusion. These are the rubber hand's visual location ($X^{\text{vis}}_{\text{rubber}}$) and the own hand's proprioceptive location ($X^{\text{prop}}_{\text{own}}$), as well as the time in which the participant sees the rubber hands' being stroked ($\tau^{\text{vis}}_{\text{rubber}}$) and felt the own hand being stroked ($\tau^{\text{tact}}_{\text{own}}$). The delay between the strokes is constant throughout

the experiment. The dynamical model captures these sensory cues as Gaussian distributions represented as follows:

$$\begin{aligned} X^{\text{vis}}_{\text{rubber}} &\sim N(\mu_{X^{\text{vis}}_{\text{rubber}}}, \sigma^2_{X^{\text{vis}}_{\text{rubber}}}) \\ X^{\text{prop}}_{\text{own}} &\sim N(\mu_{X^{\text{prop}}_{\text{own}}}, \sigma^2_{X^{\text{prop}}_{\text{own}}}) \\ \tau^{\text{vis}}_{\text{rubber}} &\sim N(\mu_{\tau^{\text{vis}}_{\text{rubber}}}, \sigma^2_{\tau^{\text{vis}}_{\text{rubber}}}) \\ \tau^{\text{tact}}_{\text{own}} &\sim N(\mu_{\tau^{\text{tact}}_{\text{own}}}, \sigma^2_{\tau^{\text{tact}}_{\text{own}}}) \end{aligned} \tag{1}$$

The locations of the hands (X) are in mm, and the time when the seen and felt stoking happens (τ) are in $msec$. In the model the mean of the seen stroking ($\mu_{\tau^{\text{vis}}_{\text{rubber}}}$) is set at 0, while the mean of the felt stroke ($\mu_{\tau^{\text{tact}}_{\text{own}}}$) indicates the delay between the strokes.

3.1.2 Estimation of the rubber hand

Explanation *The visual signal from the rubber hand is compared to the pre-existing model of the own hand. The comparison output is the visual estimate of the rubber hand location.*

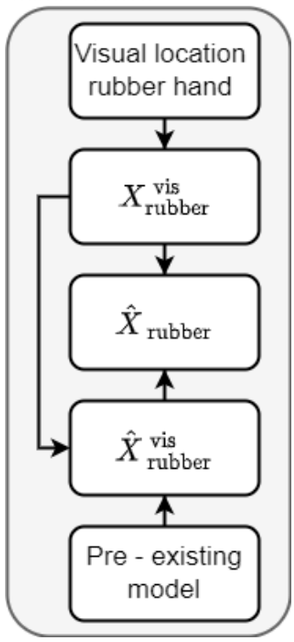

Figure 6: Visualization of how the different blocks relate to each other to estimate the location of the rubber hand ($\hat{X}_{\text{rubber}}$)

Before the experiment starts, the participant makes a first critical comparison by comparing the visual form of the rubber hand against a pre-existing model. The pre-existing model contains a reference description of the body's visual, anatomical, and structural properties. It also contains representations about (a) the shape and contours of the human body, (b) a detailed plan of the body surface, and (c) the location of body parts, the boundaries between them, and their internal part-relation [10].

The comparison between the visual form of the hand and the pre-existing model predicts that the more the viewed object matches the structural appearance of the body part's form, the stronger the illusion will be. For example, replacing the rubber hand with and non-corporeal object, such as a cardboard box, decreases the possibility of receiving the illusion [5].

The participant makes a second comparison based on the postural and anatomical features of the rubber hand. This comparison relates mainly to the postural configuration between the own and rubber hand. If the rubber hand is rotated 180°, the illusion will be less likely to arise. [10]

In the model, the results of the comparisons between the visual form of the own hand and the rubber hand determine the variance of the internal visual signal of the rubber hand ($\hat{X}^{\text{vis}}_{\text{rubber}}$). This signal is a Gaussian distribution. The model takes the average of the external and internal representation of the rubber hand's location, resulting in the final estimation of the rubber hand ($\hat{X}_{\text{rubber}}$).

Implementation into the model The model's proprioceptive drift and onset time rely on the rubber and own hands' estimated variance, which Section 3.1.4 explains. When there is a mismatch between the visual rubber hand ($X^{\text{vis}}_{\text{rubber}}$) and the pre-existing model, the illusion is less likely to arise. The model should then rely less on the visual location of the rubber hand, and thus the variance should increase.

In the model, a Gaussian distribution represents the comparisons between the visual form of the hand and the pre-existing model. This Gaussian distribution is the internal visual signal of the rubber hand ($\hat{X}^{\text{vis}}_{\text{rubber}}$). A larger variance in the Gaussian distribution relates to a more considerable mismatch between the visual form of the hand and the pre-existing model. The mean of the $\hat{X}^{\text{vis}}_{\text{rubber}}$ is similar to the location of the rubber hand $\mu_{X^{\text{vis}}_{\text{rubber}}}$.

Then the model combines the $X^{\text{vis}}_{\text{rubber}}$ and $\hat{X}^{\text{vis}}_{\text{rubber}}$ to estimate the location of the rubber hand ($\hat{X}_{\text{rubber}}$). Based on the assumption that the $X^{\text{vis}}_{\text{rubber}}$ and $\hat{X}^{\text{vis}}_{\text{rubber}}$ are measurements of the same quantity [24], the location of the rubber hand ($\hat{X}_{\text{rubber}}$) is the average between the two. Since both the $X^{\text{vis}}_{\text{rubber}}$ and $\hat{X}^{\text{vis}}_{\text{rubber}}$ are normally distributed, their average is also a Gaussian random variable. (Equation 2)

$$\begin{aligned} \mu_{\hat{X}_{\text{rubber}}} &= \frac{\mu_{X^{\text{vis}}_{\text{rubber}}} + \mu_{\hat{X}^{\text{vis}}_{\text{rubber}}}}{2} \\ \sigma^2_{\hat{X}_{\text{rubber}}} &= \frac{\sigma^2_{X^{\text{vis}}_{\text{rubber}}} + \sigma^2_{\hat{X}^{\text{vis}}_{\text{rubber}}}}{2^2} \end{aligned} \tag{2}$$

3.1.3 Calculating the perceived asynchrony

Explanation *The perceived delay between the strokes is calculated as the overlap between the seen and felt Gaussian distributions, which indicate the delay between the strokes.*

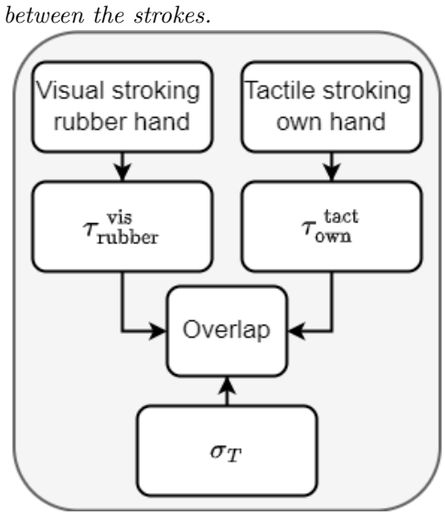

Figure 7: Visualization of how the different blocks relate to each other to estimate the perceived asynchrony (Overlap)

Once the experiment starts, the participant makes the third comparison. They compare the seen and felt stroking, and their temporal resolution of multisensory perception [10]. This temporal resolution is the individuals' sensitivity to perceive

asynchrony during the stimulation [23]. This principle is also called the temporal binding window. The larger the perceived asynchrony during the stimulation, the less likely the illusion is to arise.

The model describes perceived asynchrony as the fraction of overlap between the Gaussian distributions of the seen ($\tau^{\text{vis}}_{\text{rubber}}$) and felt ($\tau^{\text{tact}}_{\text{own}}$) stroking. This overlap fraction depends on the delay between the strokes and the variance of the Gaussian distributions. The variance is linearly related to the temporal binding window. The mean of the seen stroking ($\mu_{\tau^{\text{vis}}_{\text{rubber}}}$) is fixed at zero and the mean of the felt stroking ($\mu_{\tau^{\text{tact}}_{\text{own}}}$) indicated the delay between the strokes, which is constant during the experiment.

Implementation into the model To implement the perceived asynchrony into the model, the model assumes that it is similar to the fraction of overlap of the Gaussian distributions of the seen ($\tau^{\text{vis}}_{\text{rubber}}$) and felt ($\tau^{\text{tact}}_{\text{own}}$) stroking. The model needs the mean of the seen and felt strokes, which indicates the delay between them, and their variances to calculate this fraction.

Based on research from Hirsh and Sherrick [25], the variances of the seen ($\sigma_{\tau^{\text{vis}}_{\text{rubber}}}$) and felt ($\sigma_{\tau^{\text{tact}}_{\text{own}}}$) strokes are the set to be the same (σ_{T}). The amount of variance is dependent on the individual's temporal binding window. With a higher temporal binding window, the participant can perceive larger delays between the strokes as synchronous [23]. In the model, the overlap fraction is larger with an increased temporal binding window, resulting in more perceived synchrony between the strokes. Appendix C.1 shows the derivation of the relationship between σ_{T} and the temporal binding window.

For the perceived asynchrony or the overlap fraction, three options are possible: a) There is no delay, and thus the Gaussian distributions are in total overlap (total perceived synchrony); b) the delay and temporal binding window result in no overlap at all (total perceived asynchrony) or; c) there is a delay, and the Gaussian distributions are in partial overlap (as shown in Figure 12-Temporal). The fraction overlap results in 1 or 0 for the first two options. For the third option, the model calculates the overlap fraction.

The model does this by calculating the fraction of the overlapping regions of the two Gaussian distributions. The first step in this process is finding the intersection point of the two Gaussian distributions. Because both Gaussian distributions have the same variance (σ_{T}), the intersection point is in the middle of the two distributions. In the model, $\mu_{\tau^{\text{tact}}_{\text{own}}}$ is defines as the delay between the strokes and $\mu_{\tau^{\text{vis}}_{\text{rubber}}}$ is zero. (Equation 3)

$$t = \frac{\mu_{\tau^{\text{vis}}_{\text{rubber}}} + \mu_{\tau^{\text{tact}}_{\text{own}}}}{2} \tag{3}$$

Since the Gaussian distributions of the visual and tactile cues are similar, it is possible to normalize them. Then the area of both distributions is equal to one, and the area of the tactile Gaussian distribution below the intersection point is equal to the p-value. The p-value is found by calculating the z-score and using the Z-table.

$$Z = \frac{t - \mu_{\tau^{\text{tact}}_{\text{own}}}}{\sigma_{\text{T}}} \tag{4}$$

The overlap fraction is then calculated as the total probability area divided by the total area, which is the total of two normalized distributions minus the total probability area.

$$\begin{aligned} \text{Overlap} &= \frac{2 * 1 * \text{p}(\tau^{\text{tact}}_{\text{own}} < t)}{2 * 1 - \text{p}(\tau^{\text{tact}}_{\text{own}} < t) * 1 * 2} \\ \text{Overlap} &= \frac{\text{p}(\tau^{\text{tact}}_{\text{own}} < t)}{1 - \text{p}(\tau^{\text{tact}}_{\text{own}} < t)} \end{aligned} \tag{5}$$

3.1.4 Dynamic estimation of the own hand location

Explanation *The proprioceptive location of the own hand is compared to the constantly updating internal predicted location of the own hand. The comparison output is the proprioceptive estimate of the own hand location.*

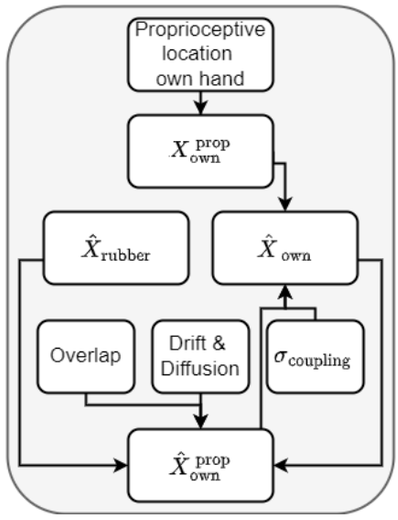

Figure 8: Visualization of how the different blocks relate to each other to estimate the location of the own hand ($\hat{X}_{\text{own}}$)

After finding the estimated location of the rubber hand and the perceived asynchrony between the stroking, it is time to estimate the location of the own hand. The estimated location of the own hand ($\hat{X}_{\text{own}}$) is modeled as the complete Bayesian fusion between the external location of the own hand ($X^{\text{prop}}_{\text{own}}$) and an internal predicted location of the own hand ($\hat{X}^{\text{prop}}_{\text{own}}$). These are all Gaussian distributions. The ability to combine the external and internal cues differ between individuals [26]. Therefore, a coupling prior (σ_{coupling}) is added to the weighting factors of the Bayesian integration.

To make this model dynamic, the internal predicted location of the own hand ($\hat{X}^{\text{prop}}_{\text{own}}$) is constantly updating. The updating of the $\hat{X}^{\text{prop}}_{\text{own}}$ uses the prediction step of the Kalman filter [13]. The model assumes that the internal predicted location of the own hand ($\hat{X}^{\text{prop}}_{\text{own}}(t+dt)$) is related to its current prediction $\hat{X}^{\text{prop}}_{\text{own}}(t)$ and the estimation of the rubber hand $\hat{X}_{\text{rubber}}$. This assumption is based on Van Beers et al. [27]. They showed that the estimation partly relies on the visual cue, even with a mismatch between the visual and proprioceptive senses.

The estimated location of the own hand $\hat{X}_{\text{own}}$ is a direct representation of the proprioceptive drift in the experiment. The literature shows that the proprioceptive drift is related to the (a)synchrony of the stroking [28]. As shown in the experiment, the proprioceptive drift also differs per participant. Therefore, the updating of the internal predicted location of the own hand ($\hat{X}^{\text{prop}}_{\text{own}}(t+dt)$) also depends on perceived asynchrony (Overlap) and a variable related to $\mu_{\hat{X}^{\text{prop}}_{\text{own}}}$, and $\sigma_{\hat{X}^{\text{prop}}_{\text{own}}}$, namely the drift and diffusion.

Implementation into the model The model calculates the estimation of the own hand using the Bayes rule by integrating the external location and the predicted internal location of the hand [8] (Equation 6). This integration uses weighting factors for both cues ($\omega_{X^{\text{prop}}_{\text{own}}}(t)$ and $\omega_{\hat{X}^{\text{prop}}_{\text{own}}}(t)$) and a coupling prior ($\sigma^2_{\text{coupling}}(t)$) to influence their reliability (Equation 7). The coupling prior is equal to a constant C at $t = 0$. It varies with the distance between the internal predicted location of the own hand and the estimated location (Equation 8). The coupling prior constant C scales with the participants' ability to merge internal and external signals [26].

$$\begin{aligned}\mu_{\hat{X}_{\text{own}}}(t) &= \omega_{X^{\text{prop}}_{\text{own}}}(t)\mu_{X^{\text{prop}}_{\text{own}}} + \omega_{\hat{X}^{\text{prop}}_{\text{own}}}(t)\mu_{\hat{X}^{\text{prop}}_{\text{own}}}(t)\\ \sigma_2{}_{\hat{X}_{\text{own}}(t)} &= \omega^2_{X^{\text{prop}}_{\text{own}}}(t)\sigma^2_{X^{\text{prop}}_{\text{own}}} + \omega^2_{\hat{X}^{\text{prop}}_{\text{own}}}(t)\sigma^2_{\hat{X}^{\text{prop}}_{\text{own}}}(t)\end{aligned} \tag{6}$$

$$\begin{aligned}\omega_{X^{\text{prop}}_{\text{own}}}(t) &= \frac{\sigma^2_{\hat{X}^{\text{prop}}_{\text{own}}}(t)}{\sigma^2_{X^{\text{prop}}_{\text{own}}} + \sigma^2_{\hat{X}^{\text{prop}}_{\text{own}}}(t) + \sigma^2_{\text{coupling}}(t)}\\ \omega_{\hat{X}^{\text{prop}}_{\text{own}}}(t) &= \frac{\sigma^2_{X^{\text{prop}}_{\text{own}}} + \sigma^2_{\text{coupling}}(t)}{\sigma^2_{X^{\text{prop}}_{\text{own}}} + \sigma^2_{\hat{X}^{\text{prop}}_{\text{own}}}(t) + \sigma^2_{\text{coupling}}(t)}\end{aligned} \tag{7}$$

$$\sigma^2_{\text{coupling}}(t+dt) = C + \frac{\mu_{\hat{X}^{\text{prop}}_{\text{own}}}(t=0) - \mu_{\hat{X}_{\text{own}}}(t)}{\mu_{\hat{X}_{\text{own}}}(t=0) - \mu_{\hat{X}_{\text{rubber}}}(t=0)} * C \tag{8}$$

In this model, the internal predicted location of the own hand ($\hat{X}^{\text{prop}}_{\text{own}}$) updates constantly. The model assumes that the updating of this prediction involves the estimated location of the rubber hand ($\hat{X}_{\text{rubber}}$), based on research of Van Beers [27]. The difference between the estimated location of the rubber hand ($\hat{X}_{\text{rubber}}$) and the current predicted location of the own hand ($\hat{X}^{\text{prop}}_{\text{own}}(t)$) influence the predicted location of the own hand at the next time step ($\hat{X}^{\text{prop}}_{\text{own}}(t+dt)$). This difference is normalized by dividing it by the initial difference between the estimated location of the rubber hand ($\hat{X}_{\text{rubber}}$) and the predicted location of the own hand ($\hat{X}^{\text{prop}}_{\text{own}}(t = 0)$). This matches empirical findings related to the proprioceptive drift [29]. (Equation 9)

$$\begin{aligned}\Delta_\mu(t) &= \frac{\mu_{\hat{X}^{\text{prop}}_{\text{own}}}(t) - \mu_{\hat{X}_{\text{rubber}}}}{\mu_{\hat{X}^{\text{prop}}_{\text{own}}}(t=0) - \mu_{\hat{X}_{\text{rubber}}}}\\ \Delta^2_\sigma(t) &= \frac{\sigma^2_{\hat{X}^{\text{prop}}_{\text{own}}}(t) - \sigma^2_{\hat{X}_{\text{rubber}}}}{\sigma^2_{\hat{X}^{\text{prop}}_{\text{own}}}(t=0) - \sigma^2_{\hat{X}_{\text{rubber}}}}\end{aligned} \tag{9}$$

The updating of the $\hat{X}^{\text{prop}}_{\text{own}}$ results in an updated estimated location of the own hand $\hat{X}_{\text{own}}$, which is directly related to the proprioceptive drift. The influence of the perceived asynchrony (Overlap) and individual differences (Drift and Diffusion) on the proprioceptive drift are included in the updating process of the predicted location of the own hand $\hat{X}^{\text{prop}}_{\text{own}}(t+dt)$. (Equation 10)

$$\begin{aligned}M &= \text{Drift} + \text{Drift} * \text{Overlap}\\ V &= \text{Diffusion} + \text{Diffusion} * \text{Overlap}\end{aligned} \tag{10}$$

Using both Equation 9 and 10 the equation for the updating of the of internal predicted location of the own hand ($\hat{X}^{\text{prop}}_{\text{own}}$) is calculated. It uses the internal predicted location of the own hand ($\hat{X}^{\text{prop}}_{\text{own}}(t)$) and the difference between the estimated location of the rubber hand ($\hat{X}_{\text{rubber}}$) and the current predicted location of the own hand ($\hat{X}^{\text{prop}}_{\text{own}}(t)$). This is influenced by the Drift, Diffusion and Overlap, and is used to calculate the internal predicted location of the own hand at the next time step ($\hat{X}^{\text{prop}}_{\text{own}}(t+dt)$). (Equation 11)

$$\begin{aligned}\mu_{\hat{X}^{\text{prop}}_{\text{own}}}(t+dt) &= \mu_{\hat{X}^{\text{prop}}_{\text{own}}}(t) - \Delta_\mu(t) * M * dt\\ \sigma_{\hat{X}^{\text{prop}}_{\text{own}}}(t+dt) &= \sigma_{\hat{X}^{\text{prop}}_{\text{own}}}(t) + \Delta_\sigma(t) * V * dt\end{aligned} \tag{11}$$

In this equation, the minus in the formula for the $\mu_{\hat{X}^{\text{prop}}_{\text{own}}}(t+dt)$ indicates a drift towards the rubber hand. This minus is due to how the rubber and own hand's location are defined in the model.

3.1.5 Perceiving the illusion

Explanation *The difference between the predicted internal location of the own hand and the estimated location of the rubber hand reaches a threshold. The intersection of the threshold with this distribution is the probability of perceiving the illusion.*

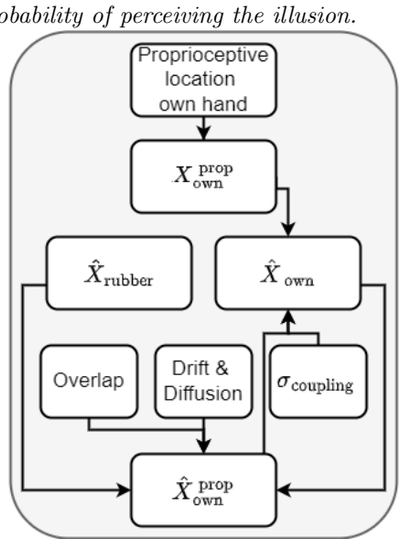

Figure 9: Visualization of how the different blocks relate to each other to perceive the illusion at a certain time (onset)

Besides the proprioceptive drift, researchers also quantify the illusion with the onset time, which is the time it takes to perceive the hand as one's own [16]. For the onset time, the participant unconsciously perceives the illusion at a particular time point. Researchers believe that the onset time is related to the sensation of ownership [30] or the referral of touch sensation [31].

Results from the experiment show no significant correlation between the onset time and the ownership in both the synchronous and the asynchronous conditions, only for the synchronous condition. This result is the same between the onset time and the proprioceptive drift. Therefore, the model assumes that the onset time is related to a higher level in the hierarchy mentioned in Section 3.1.1. Here, this higher level is the difference between the predicted internal location of the own hand $\hat{X}^{\text{prop}}_{\text{own}}$ and the estimated location of the rubber hand $\hat{X}_{\text{rubber}}$.

The difference between the predicted internal location of the own hand $\hat{X}^{\text{prop}}_{\text{own}}$ and the estimated location of the rubber hand $\hat{X}_{\text{rubber}}$ is a Gaussian distribution that differs over time $\hat{X}_{\text{diff}}(t)$. I assume that once the $\hat{X}_{\text{diff}}(t)$ reaches a threshold, the participant unconsciously decides that the rubber hand is his/her own. Due to the differences in proprioceptive drift and the given onset time between participants, the model assumes that the threshold height is participant-specific. Over time the proprioceptive drift needed before pressing the onset

time button decreases (Table 1), suggesting that the threshold declines over time.

Implementation into the model The model uses the difference between the predicted internal location of the own hand $\hat{X}_{\text{own}}^{\text{prop}}$ and the estimated location of the rubber hand $\hat{X}_{\text{rubber}}$. Once this Gaussian distribution ($\hat{X}_{\text{diff}}$) reaches a threshold, the intersection point represents the probability of receiving the illusion at that time point.

The model uses standard Gaussian rules to calculate the difference between the $\hat{X}_{\text{own}}^{\text{prop}}$ and the $\hat{X}_{\text{rubber}}$ (Equation 12). It also uses a linear formula for the threshold (Equation 13). The threshold's height and decline are participant-specific.

$$\begin{aligned} \mu_{\hat{X}_{\text{diff}}}(t) &= \mu_{\hat{X}_{\text{own}}^{\text{prop}}}(t) - \mu_{\hat{X}_{\text{rubber}}} \\ \sigma_{\hat{X}_{\text{diff}}}(t) &= \sigma_{\hat{X}_{\text{own}}^{\text{prop}}}(t) + \sigma_{\hat{X}_{\text{rubber}}} \end{aligned} \tag{12}$$

$$Threshold = \text{height} - \text{decline} * dt * \text{Overlap} \tag{13}$$

Once the $\hat{X}_{\text{diff}}$ reaches the threshold at a certain time point, the model calculates the probability that the threshold is equal to the $\hat{X}_{\text{diff}}$. Doing this for every time step results in the probability function of the onset time. (Equation 14)

$$\text{Onset}(t) = \text{p}(\hat{X}_{\text{diff}}(t) = \text{Threshold}(t)) \tag{14}$$

3.1.6 Simulation

An app with realistic parameters calculates the proprioceptive drift and the onset time with the equations above and visualizes them in graphs (Figure 12). The app uses typical distances between the hands (0-60 cm) and normal temporal delays between the strokes (0-1000 msec) for the external signals. The stimulation uses a distance of 15 cm between the hands. The variance of the proprioception ($\sigma^2_{X_{\text{own}}^{\text{prop}}}$) was set to 15 mm [9]. The variance of the visual location of the rubber hand ($\sigma^2_{X_{\text{rubber}}^{\text{vis}}}$) is 1 mm, corresponding results from literature [9]. The delay between the stroking is 0 msec for synchronous stroking and 500 msec for asynchronous stroking.

Besides the external signals, the parameters for the internal variables (temporal binding window, coupling prior constant, drift, diffusion, onset height, and decline) have also been set. Table 11 in Appendix D shows an overview, and Section 3.3 explanations of the ranges of the variables.

3.2 Results

Figures 10 and 11 show the simulation results that results from the created app shown in Figure 12. When there is a temporal delay between the signals, in the case of asynchronous stroking, the proprioceptive drift is lower than in the synchronous condition. The onset time in the asynchronous condition arises later and is more spread. Therefore, the model can account for the rubber hand illusion.

The maximal proprioceptive drift stabilizes after a certain distance when the effect of distance between the rubber and the real hand is assessed. When the distance between the rubber and the real hand reaches zero, the drift also decreases (Figure 10). This matches findings from Erro et al. [29]. Besides that, the onset time gradually vanishes as the distance between the hands approaches 30 cm when the height of the onset threshold is at its maximum. This implies that the illusion vanishes when the distance between the hands is larger than 30 cm. These results closely match empirical findings, which had shown that the illusion deteriorates as a function of distance, and found that the spatial limits on the experience of the illusion was 27.5 cm [31]. When the distance between the hands is smaller than the threshold height, the model has no onset time. In these cases, the threshold should be decreased to match the literature.

The effect of the delay between the stroking has been assessed to further examine the model's validity (Figure 11). An increasing delay between the stoking decreases the maximal proprioceptive drift, stabilizing as the delay increases. The peak of the onset time arises later with an increasing delay between the strokes. A final effect of an increasing delay between the stroking is an increase in the total duration of the onset time. This is in line with the results of the experiment and empirical findings [17].

3.3 Effect of parameters on model behavior

Each variable has its influence on the model. Besides that, each parameter has its ranges based on the experiment's results or values from the literature. Below the influences and the ranges of each parameter are explained. For the representation, the distance between the hands is set at 15 cm for a duration of 600 seconds. Further, the model uses the initial values while only varying one of the parameters (Table 11). The graphs in Appendix D visualize the effects of each parameter.

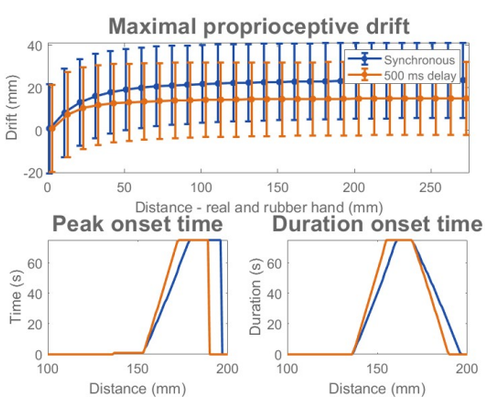

Figure 10: Simulation results: Spatial effects, increasing the distance between the seen rubber hand and the felt own hand.

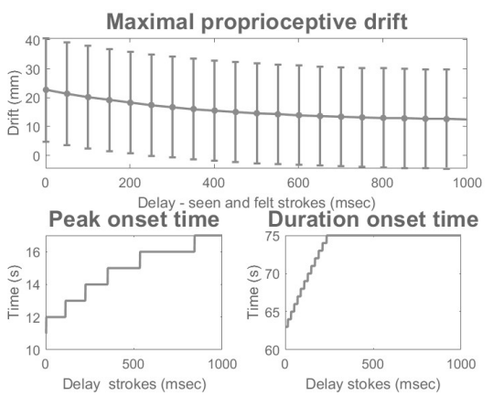

Figure 11: Simulation results: Temporal effects, increasing the delay between the seen strokes on the rubber hand and the felt strokes on the own hand

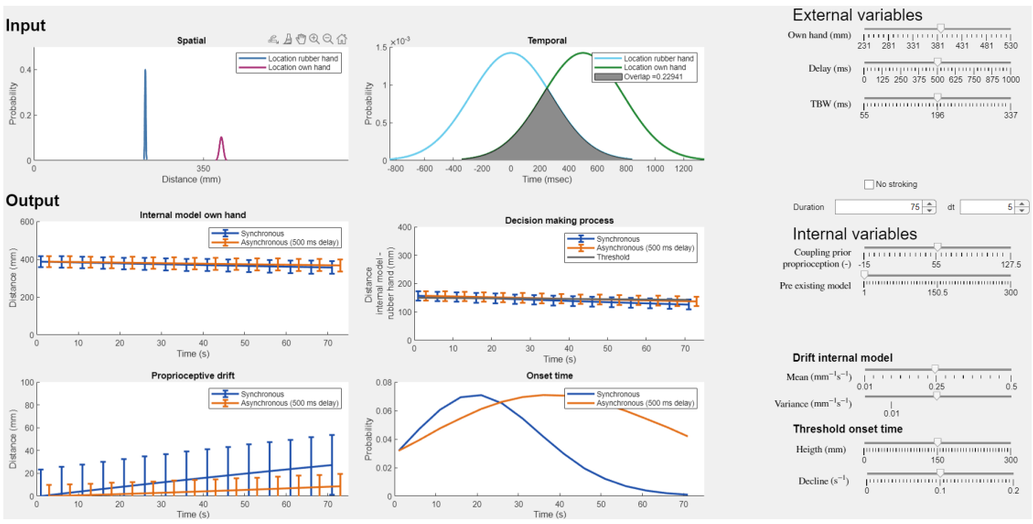

Figure 12: Visualization of the app: The spatial and temporal plot visualize the model's inputs. In the temporal plot, the user can adjust the location of the own hand with the slider of the own hand. The variance of the seen and felt stroking can be changed with the temporal binding window slider, and with the delay slider, the Gaussian distribution of the stroking of the own hand can be changed. Furthermore, the duration and the internal variables can be adjusted. Section 3.3 summarize the effects of these internal variables. In the app, only one line is visible. Here, the synchronous and asynchronous condition illustrates the difference between the two.

3.3.1 Temporal binding window (ms)

The temporal binding window affects the width of the Gaussian distributions in the temporal aspects. A higher value will result in a Gaussian distribution with a higher variance. This directly results in a higher overlap when there is a delay between the seen and felt stroking. The temporal binding window has no effect when there is no delay. The fraction of overlap in the temporal aspect is responsible for the amount of proprioceptive drift and the width of the onset time. Thus, increasing the temporal binding window when there is a delay between the felt and seen stroking will increase the proprioceptive drift and decrease the time it takes for the peak of the onset time to arise. Increasing the temporal binding window will also decrease the duration of the onset time.

The temporal binding window parameter ranges are based on the results of Constantini et al. [23]. They found that the average width of the temporal binding window was 196 ms with a standard deviation of 47 ms. To include 99.7% of all participants or three times the standard deviation results in the range of 55 to 337. The given value is linearly related to the variance of the felt and seen stroking Gaussian distributions in the model (σ_T). The mathematical derivation is in Appendix C.1.

3.3.2 Coupling prior constant ($-$)

Increasing the coupling prior constant (C) will result in more proprioceptive drift. The maximal proprioceptive drift stabilizes as the coupling prior constant increases. There is a slight difference in the maximal proprioceptive drift in synchronous and asynchronous conditions. The time of the maximal drift is different for the synchronous and asynchronous conditions. The maximal drift arises earlier in the synchronous condition. Besides the maximal drift, the prior coupling constant also influences the proprioceptive drift's variance. This variance decreases once the coupling prior constant reaches zero and then increases again with an increasing coupling prior constant. The coupling prior constant does not influence the onset time.

The coupling prior constant is directly related to the weighting factor used in the estimation of the own hand. This weighting factor is calculated using the external and internal signals variances. The variance of the external signals is set to 15, similar to Samad et al. [9], and the variance of the internal signal at t = 0 is 30. A coupling prior of -15 lets the model rely solely on the external signal to calculate the estimation of the own hand. A coupling prior of 125 lets the model rely mainly on the internal signals. These values are mathematically explained in Appendix C.2.

3.3.3 Internal model - Drift and diffusion ($mm^{-1}s^{-1}$)

Increasing the drift results in more proprioceptive drift, where the time it reaches the maximal drift differs for synchronous and asynchronous conditions. The time it takes to reach the maximal proprioceptive drift in the synchronous condition decreases as the drift increases. With an increasing drift, the time it takes to reach the peak of the onset time decreases and stabilizes. The duration of the onset time behaves similarly.

Increasing the diffusion will decrease the maximal proprioceptive drift. While the maximal variance of the proprioceptive drift increases. The duration of the onset time increases as the diffusion of the internal model increases.

The ranges of the drift and diffusion of the internal model are based on the formulas in equation 10. To change the predicted internal location of the own hand, the output of equation 10 must be greater than zero and is therefore set to 0.01. The maximal influence of the difference between the estimated location of the rubber hand ($\hat{X}_{\text{rubber}}$) and the predicted location of the own hand ($\hat{X}_{\text{own}}^{\text{prop}}$) should be 1. From this, it directly follows that the maximal value for the drift should be 0.5.

The variance of the $\hat{X}_{\text{own}}^{\text{prop}}$ is also used in the weighing factors and has more influence on the model. Therefore the diffusion ranges are ten times smaller than those of the drift.

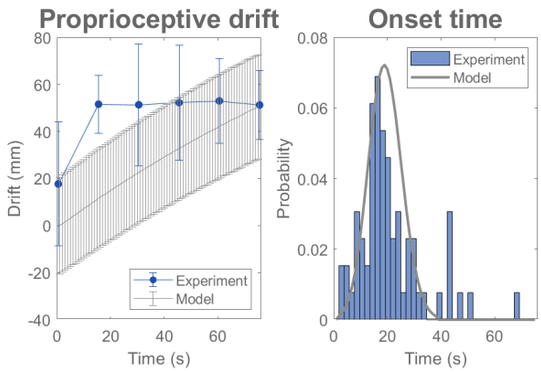

Figure 13: Best fit between the synchronous results of the experiment and the dynamic model.

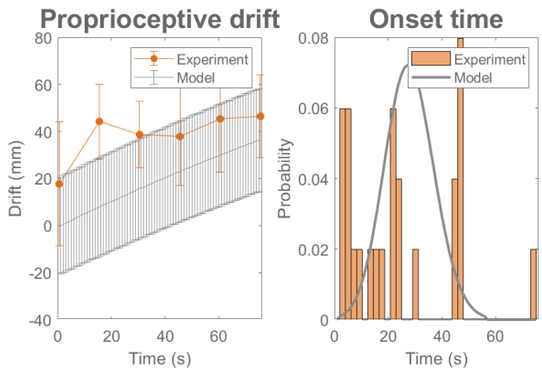

Figure 14: Best fit between the asynchronous results of the experiment and the dynamic model.

Table 4: Values of the parameters used for the best fit. The temporal binding window does not influence the results from the synchronous condition.

Condition	**Temporal binding window**	**Coupling prior constant**	**Drift**	**Diffusion**	**Height threshold**	**Decline threshold**
Best fit	337	121.8	0.5	0.001	140	0

3.3.4 Threshold onset time - Height (mm)

The height of the onset threshold and its influence on the model is dependent on the initial distance between the own and rubber hand. Once the threshold is high enough to touch the $\hat{X}_{\text{diff}}$ (Figure 12) and keeps increasing, the time it takes to reach the peak of the onset time will decrease. The onset time duration will increase until the Gaussian's mean ($\mu_{\hat{X}_{\text{diff}}}$) crosses the threshold. Then the duration of the onset time will decrease again. The height of the threshold does not influence the proprioceptive drift.

The lowest value for the height of the threshold is zero, which means that there is no difference between the position of the rubber hand and the predicted location of the own hand. The maximum value for the height is related to the spatial limit found by Lloyd [31]. The time to elicit the illusion decreases when the distance between the hands is larger than 30 cm. By setting the maximum value of the height of the threshold to 250 mm, the model generates similar onset times with a distance between the hands between 0 and 250 mm. A larger distance between the hands will result in an increased onset time, which is in line with the results of Lloyd [31].

3.3.5 Threshold onset time - Decline (s^{-1})

Increasing the decline of the onset threshold is related to an increase in the time it takes to reach the peak of the onset time. The duration of the onset time also increases with an increasing decline in the onset time. The decline of the onset threshold does not influence the proprioceptive drift.

The threshold's decline ranges are based on the experiment's results. The asynchronous condition has a non-significant correlation coefficient of 0.04. In the synchronous condition, the significant correlation is 0.45. Due to the non-significance and the fact that the onset time is not directly related to the proprioceptive drift, the ranges are 0-0.2.

3.4 Dynamical model vs Experiment

To further validate the model, I compared the results from the experiment with the model using a grid search (Figures 13 and 14). For this grid search, all possible values for the mean and variance of the proprioceptive drift and onset time are calculated using all possible parameter combinations (1.038.180). Then every parameter combination is compared with the results of the experiment. For comparing the mean and variance of the proprioceptive drift between the model and the experiment, the error sum of squares was calculated. For the onset time, the correlation between the model and participant was calculated using the function corr2 from Matlab. Then all the outcomes were normalized over the parameter options. Finally, the sum was taken from the normalized mean and variance of the proprioceptive drift and the onset time values, in which the lowest value is the best fit.

Figure 13 and 14 show the results of the comparison between the model and the results of the experiment. The proprioceptive drift arises earlier in the experiment than in the model. After 75 seconds, the proprioceptive drift from the model and the experiment are close. Furthermore, the proprioceptive drift of the experiment starts at a higher point than the model. The model can correctly predict the onset time outcomes from the experiment in the synchronous condition. In the asynchronous condition, the onset time from the experiment is more spread over time. Here, the model is less able to include all the results from the experiment. The model fails to include the onset times further away from the main distribution. Due to the lack of data for individual participants, I did not compare the model and one participant.

4 Discussion

4.1 Experiment

The experimental output consisted of three tasks: pressing the button when the illusion arises, placing a marker at the position of the own hand, and filling in a questionnaire. For pressing the button and thus finding the onset time, 25 out of 37 participants pressed the button. The onset time output is

consistent with the literature; 60-62 out of the 117 participants responded in a synchronous active and passive movement experiment from Kalckert and Ehrsson [16]. Of the 52 participants Lloyd recruited, 42 agreed in all conditions with the statement: 'It seemed as though the touch I felt was caused by the experimenter touching the rubber hand' [31].

Besides the number of responses, the average onset time for the synchronous condition (21.1 seconds) is also consistent with the literature. Kalckert and Ehrsson [16] found an average onset time of approximately 23 seconds. The presented frequency histogram in their study (Figure 4) is equivalent to the top-left graph in Figure 3. With an initial distance of 27.5 cm between the hands, Lloyd [31] found an average onset time of 15 seconds. Lane et al. [17], who also investigated the duration of the illusion, found a much higher onset time for the illusion. The onset time was approximately 100 seconds. Their results included participants who had not experienced the illusion, which explains the slower responses. The experimental setup and procedures differ in the number of responders and average onset time. This study shows that an automated setup can obtain similar onset times.

At first sight, my findings regarding the proprioceptive drift seem inconsistent with the literature. In most studies that use motor response as proprioceptive drift measurement [28, 32, 33, 34], a significant difference can be found between the synchronous and asynchronous conditions. In this study, these conditions did not significantly differ at all. The results are, however, similar to the results of Rohde et al. [35], who investigated the difference between measurement frequency in synchronous and asynchronous conditions. They found that the proprioceptive drift also occurred in the asynchronous condition in an increased measurement frequency (12x10 sec). In other groups (3x40 sec and 1x120 sec), the asynchronous stroking resulted in a significant difference, suggesting that a session has an optimum frequency of measurements. The conducted experiment probably went over this optimum.

The amount of drift in the synchronous and asynchronous conditions ($t = 75$ s, 5.1 ± 1.5 cm and 4.6 ± 1.8 cm) is larger than measurements seen in other studies which used a horizontal set-up [18, 19, 36]. They all found a 2.5-3.5 cm drift in the synchronous condition and 1-3 cm in the asynchronous condition. The results of Rohde et al. [37] are more similar to the results of this experiment; they found a drift of approximately 7 cm in the synchronous condition and 3 cm in the asynchronous condition. The results are, however, hard to compare since the experimental setup and the duration differ from the current study. In the study of Rohde et al. [35], who investigated the measurement frequency, the amount of drift seems to stabilize around 5 cm for both the synchronous and asynchronous conditions, which is in line with the results of this study.

The questions used in the questionnaire are from Riemer et al. [19]. They implemented passive tactile stimulation and active voluntary movements in their experiment. The synchronous and asynchronous conditions are significantly different for the ownership and agency items with passive tactile stimulation, while the control items were not significant. These results are similar to the presented results, but in my research, the control items also significantly differ in conditions. In non of the questions, a significant difference over time is noticeable.

Increasing the duration of the stimulation did not affect the ownership results. However, there is a significant difference over time in the proprioceptive drift, mostly related to the initial measurement. This phenomenon is in line with the results of Gallagher et al. [38], who had an increasing drift over time compared to a stable ownership questionnaire. Their study's most prolonged condition took 5 minutes, which might explain the significance of the proprioceptive drift. This study, the study of Gallagher et al. [38] and Rohde et al. all draw similar conclusions. They all suggest that a dissociation between the proprioceptive drift and the questionnaire is in place and that they reflect separate underlying processes of the illusion.

Even though the increased duration of the stimulation indicates a dissociation between the proprioceptive drift and the ownership results, direct comparisons between the two show a significant positive correlation between them. The correlation between the ownership statements in the synchronous and the asynchronous conditions are positive, but only the synchronous condition is significant. Figure 17 shows that the different routines scatter though out the graph, and the correlation between the proprioceptive drift and ownership over time is inconclusive. This is similar for the other correlations (Figures 15 and 16). Therefore no conclusions can be drawn about the correlation between the measurement methods over time.

I used an automated setup for the induction of the illusion. This setup was replicated and updated from Sivasubramaniam et al. [14]. I updated the coding to include different induction times, measurement of the onset time, filling in a questionnaire, and saving the data in the corresponding excel sheets. Besides that, I added a plate for measurements of the proprioceptive drift. Due to one of the legs of this plate, the rubber hand is not completely visible to the participant, which may influence the study results. Eliminating this possible influence is a must in a future version. Another motor could be added to the setup in further research so that the brushes rotate separately. This way, the temporal binding window could be found, and an increased delay or inconsistent stroking between the brushes can be induced.

Using an automated setup version has clear advantages over a manual setup. It is easier to compare results, and the precision of visual and tactile stimuli is much higher than manual stroking. This way, the potential error due to human limitations is decreased [14]. The downside of using an automated setup is the loss of social or empathetic factors, which are also involved in the rubber hand illusion [37].

4.2 Dynamical model

In this thesis, I proposed a dynamic model related to the rubber hand illusion's proprioceptive drift and onset time. The model includes most of the rubber hand illusion's underlying theories. The dynamical model allows interpreting the perceptual decision process in predictive coding [20], which postulates that a decision is made using a comparison of predicted and observed sensory input. The predicted sensory input is updated over time, while the observed sensory input is static. The model shows that varying the internal variables explains the experiment results of the proprioceptive drift and onset time.

The general equations are directly derived

and interpreted from the experiment results and conclusions from literature [28, 29]. The formulas of the estimation of the own hand ($\hat{X}_{\text{own}}$) are based on the Kalman filter [13] and the Bayes rule [8]. The $\hat{X}_{\text{own}}$ is directly related to the proprioceptive drift. The predicted location of the own hand ($\hat{X}_{\text{own}}^{\text{prop}}$), the result of the Kalman filter's prediction step, is later used in the process for calculating the onset time. The drift-diffusion model [21] inspires the decision-making process for the onset time. Which accumulates noisy pieces of evidence over time. The model consists of six parameters. Further research is needed to determine these parameters better and generalize these parameters using, for example, personal traits.

I based the parameter ranges on the experiment's results or values from the literature. The values based on the experiment's results may have improved ranges once an experiment is done without reaching the optimum number of conditions. This experiment might lead to better results and improve the ranges of the parameters.

The presented model is related to previous models of the rubber hand illusion. For example, Samad et al. [9] adopted the Bayesian causal inference model of multisensory perception. They applied it to visual, proprioceptive, and tactile stimuli. They showed that their model could reproduce the rubber hand illusion but failed to show the dynamics and interpersonal differences of the illusion. Tsakiris et al. [10] included the interpersonal differences in their model but only mentioned the comparisons made during the illusion rather than concrete formulas for the illusion. The literature has not yet presented another model related to the dynamics of the rubber hand illusion. The presented model has the advantage that it shows the dynamics of the illusion and compares the external signals proposed by Samad et al. [9] and includes interpersonal differences as presented by Tsakiris et al. [10].

The model contains additional constraints to decrease the number of parameters to six. Without these constraints, the model would have had ten parameters. I constrained four parameters that relate to the external signals. These are the means of the seen stroking, the seen location of the rubber hand, and the variances of the rubber and own hand's locations. I based the constraints on the results of van beers et al. [22] and Jones et al. [39]. Who found that the variability of the visuals is around 0.36 degrees [22], which, with an eye-rubber hand distance of 35-45 cm, translates to a standard deviation of 1 mm [9]. For the proprioception, the standard deviation was set to 15 mm [22, 39, 9]. Arguably, these values vary per participant and per condition. A less illuminated environment would result in a higher visual variance than a more illuminated environment. The model ignores these external factors for simplicity and the literature's lack of data.

The dynamical model can be used to investigate novel experimental questions. For example, as suggested by Rohde et al. [35] and the results of this study, there could be an optimum amount of measurements in a session for the proprioceptive drift. This optimum limits the experimenter in finding the dynamics of the proprioceptive drift. The proprioceptive drift of other time points can be found using this model and decreasing the measurements. Besides predicting results from an experiment, it could be used for post-stroke rehabilitation or in the use of robotic devices. These fields are, however, not mature yet [7]. This model could be a step maturing process of these fields.

4.2.1 Extensions

The current model is a simplified version to explain the dynamics of the rubber hand illusion. More research increases the model's accuracy. This research should focus on the parameter formulas and possible additional model components to make it more applicable. This section discusses the possible improvements and extensions of the presented model.

The first improvement is looking into the possibility of having the hand at the same distance, for example, in the case of virtual reality [40] or with amputees [41]. Due to the current formulas used, the model gives errors when the location of the rubber hand and the own hand are the same. No proprioceptive drift is possible in these cases, but the feeling of ownership can still arise. I did not develop formulas related to the feeling of ownership due to the unknown relationship between the proprioceptive drift, onset time, and the feeling of ownership.

Two parameters introduced in the formulas related to the predicted location of the own hand ($\hat{X}_{\text{own}}^{\text{prop}}$) (Equations 10 and 11) vary not only with the given input but also with the amount over synchrony of the stroking. The main objective of these formulas is that the amount of drift and diffusion is related to the amount of synchrony between the strokes. Comparing the model's results with values in literature [28, 33, 38] suggests that the influence of stroking is, in reality, higher than in the proposed formulas.

The incorrect influence of the temporal aspects on the proprioceptive drift is also visible in the onset time prediction. In the asynchronous condition, it takes longer to receive the illusion, which is in line with literature [17], and the probability is similar to the synchronous condition. The probability of receiving the illusion in the asynchronous condition is lower, as shown in the performed experiment (Section 2.2). More research is needed to formulate better the influence of the temporal aspects of the illusion.

As mentioned before, this model could be used to predict results from an experiment. From the first introduction of the rubber hand illusion experiment [3], researchers investigate the strength of the illusion with a questionnaire. These questionnaires mainly consist of questions related to body ownership and agency, which I also used in this experiment. The suggested dissociation between the proprioceptive drift and the questionnaire and suggested separation of the underlying processes of the illusion [35, 38] prohibited an attempt to include it in the proposed model. More knowledge about the relationship between the proprioceptive drift and body ownership and agency is essential before implementing this element into the model. If there is no relation, more research is needed to find the underlying processes in body ownership and agency.

Riemer et al. [4] analyzed the methodological differences in the rubber hand illusion and found many differences between experimental setups in studies and induction types. The researcher integrated some differences into the model. These differences relate to the distance between the hand and the amount of synchrony between the strokes. The distance between the hands is currently on the horizontal axis. In literature, a vertical [28] or distal [34] set up have also been used for the induction of the illusion. The reliability of the visual and proprioceptive senses for the location of the hand

differ in these directions [22]. This directly results in different proprioceptive drift and onset times in these directions. Incorporating these other axes into the model might extend it to a 3D version.

Researchers can use different measurements for the proprioceptive drift: perceptual and motor responses. A study done by Kalckert and Ehrsson [42] showed a difference in measurement method for the perceived location of the hand in the method used. The stimulation type (tactile, passive, or active movements) also influences the illusion results. Using the results from Tsakiris et al. [43] could give more insight into incorporating this into the model to predict the experiment's results. For an even further advanced dynamical model related to the rubber hand illusion experiment, the properties of the induction method (tactile [44], or active movement [4]), the number and type of fingers used in the illusion [4], and the difference between an automatic or manual set up [35] could be incorporated.

Extensions in clinical applications

The model could also be used in clinical applications, but it should be adjusted to meet its needs. For example, if the model is used in pathology, one must incorporate the effects of specific deceases. Schizophrenic patients demonstrate a faster onset of the illusion than healthy patients [7]. Other pathologies have different effects, and incorporating this in the model will precisely predict pathology's effect on the rubber hand illusion. These differences are related to internal variables and might be hard to investigate.

Besides implementing the model with psychiatric disorders, the model could also be used to design neuroprosthetics [1]. The illusion in amputees is much less vivid than in the traditional rubber hand illusion. This model alone would not be sufficient to satisfy the amputee with the prosthesis. Other models with tactile sensors and stimulators are needed to reproduce and maintain the illusion [1]. With extensions related to tactile sensors and stimulators, the developers might be able to predict the satisfaction of the prosthesis before experimenting with it on amputees.

4.3 Comparison

Validating the model with a comparison between the results of the model and the results of the experiment suggests that the optimization technique used might not be good enough. A often used method for this is with Monte Carlo simulations [9, 21, 45]. For this comparison, I coded and performed a grid search with a total of 1.038.180 parameter combinations. I compared these combinations with the experiment's results using the error sum of squares for the proprioceptive drift and the correlation coefficient for the onset time for the experiment results. The scaled and summed results show the closeness of fit between the experiment and the model. The option with the lowest number is the best fit. Due to the limited number of responses, I could not validate the model with the results of the individual participants.

While this grid search method does a complete search for the given set, it has the advantage over the random search and the genetic algorithm to guarantee the best results [46]. A drawback of this method is the constraint on the testable number of combinations. For example, I used a step size of 5 mm for the height of the onset threshold. Decreasing this step size will lead to better results for the onset time but will increase the number of combinations above the file size Matlab can work with. Using another optimization technique might lead to better results.

More data from one individual must be obtained for the onset time to compare the dynamic model with individuals. A total of four presses, the maximum number of presses in the synchronous and asynchronous condition, is not enough to find a good fit between the model and the individual. Conducting more experiments with one participant over multiple days might be the solution to not exceed the measurement frequency but takes more time. It is, however, also possible that participants do not experience the illusion and do not press the onset button at all. In these cases, the current grid search cannot correctly match the onset time. I, therefore, suggest that another optimization technique should be used to match the model to the experiment's data.

The results from the best fit (Figures 13 and 14) show that the proprioceptive drift from the experiment starts at a higher point than the model. In the dynamical model, the proprioceptive drift cannot start at a different point than zero. In articles, the proprioceptive drift is calculated as the difference between pre-and post-testing [18, 35, 36]. Here, the proprioceptive drift is the difference between the hand's location and the dots on the foil. More research is needed into the initially felt location of the own hand to improve the model.

5 Conclusion

The within-subject rubber hand illusion experiment was performed to investigate the dynamics of the multisensory integration during the illusion. The experiment measured the onset time, the proprioceptive drift, the body ownership, and agency. Using different time points (15, 30, 45, 60, and 75 seconds) in either a synchronous or asynchronous condition (500 ms delay) made it possible to find the dynamics of the embodiment. Concluded from the experiment, participants are more likely to perceive the rubber hand as their own in the synchronous condition than in the asynchronous condition. In this experiment, the proprioceptive drift does, and the ownership statements do not significantly differ over time. The proprioceptive drift does not, and the ownership statements differ significantly between the synchronous and asynchronous conditions. Furthermore, the different measurements, the onset time, the proprioceptive drift, and the ownership correlate significantly in the synchronous condition but not in the asynchronous condition. The results are, however, noisy and thus overall inconclusive.

Besides this experiment, a mathematical model describing the dynamics of the multisensory integration during the rubber hand illusion is developed. Using the experiment's results and empirical findings from the literature, this model can replicate the proprioceptive drift and onset time using the Kalman filter and the Bayes rule. It fails to include ownership over the hand due to the unknown relationship between the outputs. The external inputs, the distance between the hands, and the delay in stroking can be changed to match the performed experiment. The influence of the delay between the stroking in the model is insufficient and should be improved. The dynamical model visualizes a broad spectrum of rubber hand illusion-related phenomena but is far from finished.

References

[1] H. Ramakonar, E. A. Franz, and C. R. Lind, "The rubber hand illusion and its application to clinical neuroscience," *Journal of Clinical Neuroscience*, vol. 18, no. 12, p. 1596–1601, Dec. 2011. [Online]. Available: https://linkinghub.elsevier.com/retrieve/pii/S0967586811003201

[2] M. Kammers, F. de Vignemont, L. Verhagen, and H. Dijkerman, "The rubber hand illusion in action," *Neuropsychologia*, vol. 47, no. 1, pp. 204–211, Jan. 2009. [Online]. Available: https://linkinghub.elsevier.com/retrieve/pii/S0028393208003254

[3] M. Botvinick and J. Cohen, "Rubber hands 'feel' touch that eyes see," *Nature*, vol. 391, no. 6669, pp. 756–756, Feb. 1998. [Online]. Available: http://www.nature.com/articles/35784

[4] M. Riemer, J. Trojan, M. Beauchamp, and X. Fuchs, "The rubber hand universe: On the impact of methodological differences in the rubber hand illusion," *Neuroscience & Biobehavioral Reviews*, vol. 104, pp. 268–280, Sep. 2019. [Online]. Available: https://linkinghub.elsevier.com/retrieve/pii/S014976341930051X

[5] J. Hohwy and B. Paton, "Explaining Away the Body: Experiences of Supernaturally Caused Touch and Touch on Non-Hand Objects within the Rubber Hand Illusion," *PLoS ONE*, vol. 5, no. 2, p. e9416, Feb. 2010. [Online]. Available: https://dx.plos.org/10.1371/journal.pone.0009416

[6] N. Barnsley, J. McAuley, R. Mohan, A. Dey, P. Thomas, and G. Moseley, "The rubber hand illusion increases histamine reactivity in the real arm," *Current Biology*, vol. 21, no. 23, pp. R945–R946, Dec. 2011. [Online]. Available: https://linkinghub.elsevier.com/retrieve/pii/S0960982211012000

[7] O. Christ and M. Reiner, "Perspectives and possible applications of the rubber hand and virtual hand illusion in non-invasive rehabilitation: Technological improvements and their consequences," *Neuroscience Biobehavioral Reviews*, vol. 44, p. 33–44, Jul. 2014. [Online]. Available: https://linkinghub.elsevier.com/retrieve/pii/S0149763414000621

[8] D. Meijer and U. Noppeney, "Computational models of multisensory integration," in *Multisensory Perception*. Elsevier, 2020, pp. 113–133. [Online]. Available: https://linkinghub.elsevier.com/retrieve/pii/B978012812492500005X

[9] M. Samad, A. J. Chung, and L. Shams, "Perception of Body Ownership Is Driven by Bayesian Sensory Inference," *PLOS ONE*, vol. 10, no. 2, p. e0117178, Feb. 2015. [Online]. Available: https://dx.plos.org/10.1371/journal.pone.0117178

[10] M. Tsakiris, "My body in the brain: A neurocognitive model of body-ownership," *Neuropsychologia*, vol. 48, no. 3, pp. 703–712, Feb. 2010. [Online]. Available: https://linkinghub.elsevier.com/retrieve/pii/S002839320900390X

[11] K. P. Körding and D. M. Wolpert, "Bayesian integration in sensorimotor learning," *Nature*, vol. 427, no. 6971, pp. 244–247, Jan. 2004. [Online]. Available: http://www.nature.com/articles/nature02169

[12] H. Colonius and A. Diederich, "Formal models and quantitative measures of multisensory integration: a selective overview," *European Journal of Neuroscience*, vol. 51, no. 5, pp. 1161–1178, Mar. 2020. [Online]. Available: https://onlinelibrary.wiley.com/doi/10.1111/ejn.13813

[13] R. E. Kalman, "A new approach to linear filtering and prediction problems," *Transactions of the ASME–Journal of Basic Engineering*, vol. 82, no. Series D, pp. 35–45, 1960.

[14] A. K. Sivasubramaniam, J.-H. Ng, H. Chan, J. K. Y. Yang, and A. Kalckert, "The super-stroker—an open-source tool to induce the rubber hand illusion," *Psychology of Consciousness: Theory, Research, and Practice*, pp. 1–10, Jun. 2021. [Online]. Available: http://doi.apa.org/getdoi.cfm?doi=10.1037/cns0000284

[15] O. Perepelkina, V. Vorobeva, O. Melnikova, G. Arina, and V. Nikolaeva, "Artificial hand illusions dynamics: Onset and fading of static rubber and virtual moving hand illusions," *Consciousness and Cognition*, vol. 65, pp. 216–227, Oct. 2018. [Online]. Available: https://linkinghub.elsevier.com/retrieve/pii/S1053810018302599

[16] A. Kalckert and H. H. Ehrsson, "The Onset Time of the Ownership Sensation in the Moving Rubber Hand Illusion," *Frontiers in Psychology*, vol. 8, Mar. 2017. [Online]. Available: http://journal.frontiersin.org/article/10.3389/fpsyg.2017.00344/full

[17] T. Lane, S.-L. Yeh, P. Tseng, and A.-Y. Chang, "Timing disownership experiences in the rubber hand illusion," *Cognitive Research: Principles and Implications*, vol. 2, no. 1, p. 4, Dec. 2017. [Online]. Available: http://cognitiveresearchjournal.springeropen.com/articles/10.1186/s41235-016-0041-4

[18] R. Zopf, G. Savage, and M. A. Williams, "Crossmodal congruency measures of lateral distance effects on the rubber hand illusion," *Neuropsychologia*, vol. 48, no. 3, pp. 713–725, Feb. 2010. [Online]. Available: https://linkinghub.elsevier.com/retrieve/pii/S0028393209004357

[19] M. Riemer, X. Fuchs, F. Bublatzky, D. Kleinböhl, R. Hölzl, and J. Trojan, "The rubber hand illusion depends on a congruent mapping between real and artificial fingers," *Acta Psychologica*, vol. 152, pp. 34–41, Oct. 2014. [Online]. Available: https://linkinghub.elsevier.com/retrieve/pii/S0001691814001711

[20] M. A. Apps and M. Tsakiris, "The free-energy self: A predictive coding account of self-recognition," *Neuroscience Biobehavioral Reviews*, vol. 41, p. 1432–1438, Apr. 2014. [Online]. Available: https://linkinghub.elsevier.com/retrieve/pii/S0149763413000420

[21] S. Bitzer, H. Park, F. Blankenburg, and S. J. Kiebel, "Perceptual decision making: Drift-diffusion model is equivalent to a bayesian model," *Frontiers in Human Neuroscience*, vol. 8, no. 102, pp. 1–19, Feb. 2014. [Online]. Available: http://journal.frontiersin.org/article/10.3389/fnhum.2014.00102/abstract

[22] R. J. v. Beers, A. C. Sittig, and J. J. D. van der Gon, "The precision of proprioceptive position sense," *Experimental Brain Research*, vol. 122, no. 4, pp. 367–377, Oct. 1998. [Online]. Available: http://link.springer.com/10.1007/s002210050525

[23] M. Costantini, J. Robinson, D. Migliorati, B. Donno, F. Ferri, and G. Northoff, "Temporal limits on rubber hand illusion reflect individuals' temporal resolution in multisensory perception," *Cognition*, vol. 157, p. 39–48, Dec. 2016. [Online]. Available: https://linkinghub.elsevier.com/retrieve/pii/S0010027716302001

[24] D. S. Lemons and P. Langevin, "Expected values," in *An Introduction to Stochastic Processes in Physics: Containing "On the Theory of Brownian Motion*, 2002, pp. 7–16.

[25] I. J. Hirsh and C. E. Sherrick, "Perceived order in different sense modalities," *Journal of Experimental Psychology*, vol. 62, no. 5, pp. 423–432, Nov. 1961. [Online]. Available: http://doi.apa.org/getdoi.cfm?doi=10.1037/h0045283

[26] M. Tsakiris, A. Tajadura-Jiménez, and M. Costantini, "Just a heartbeat away from one's body: Interoceptive sensitivity predicts malleability of body-representations." *Proceedings of the Royal Society B: Biological Sciences*, vol. 278, no. 1717, pp. 2470–2476, Aug. 2011. [Online]. Available: https://royalsocietypublishing.org/doi/10.1098/rspb.2010.2547

[27] R. J. van Beers, D. M. Wolpert, and P. Haggard, "When Feeling Is More Important Than Seeing in Sensorimotor Adaptation," *Current Biology*, vol. 12, no. 10, pp. 834–837, May 2002. [Online]. Available: https://linkinghub.elsevier.com/retrieve/pii/S0960982202008369

[28] A. Kalckert and H. H. Ehrsson, "The spatial distance rule in the moving and classical rubber hand illusions," *Consciousness and Cognition*, vol. 30, pp. 118–132, Nov. 2014. [Online]. Available: https://linkinghub.elsevier.com/retrieve/pii/S1053810014001603

[29] R. Erro, A. Marotta, and M. Fiorio, "Proprioceptive drift is affected by the intermanual distance rather than the distance from the body's midline in the rubber hand illusion," *Attention, Perception, Psychophysics*, vol. 82, no. 8, p. 4084–95, Nov. 2020. [Online]. Available: https://link.springer.com/10.3758/s13414-020-02119-7

[30] H. H. Ehrsson, C. Spence, and R. E. Passingham, "That's My Hand! Activity in Premotor Cortex Reflects Feeling of Ownership of a Limb," *Science*, vol. 305, no. 5685, pp. 875–877, Aug. 2004. [Online]. Available: https://www.science.org/doi/10.1126/science.1097011

[31] D. M. Lloyd, "Spatial limits on referred touch to an alien limb may reflect boundaries of visuo-tactile peripersonal space surrounding the hand," *Brain and Cognition*, vol. 64, no. 1, pp. 104–109, Jun. 2007. [Online]. Available: https://linkinghub.elsevier.com/retrieve/pii/S0278262606002119

[32] M. V. Sanchez-Vives, B. Spanlang, A. Frisoli, M. Bergamasco, and M. Slater, "Virtual hand illusion induced by visuomotor correlations," *PLoS ONE*, vol. 5, no. 4, pp. 1–6, Apr. 2010. [Online]. Available: https://dx.plos.org/10.1371/journal.pone.0010381

[33] Y. Sato, T. Kawase, K. Takano, C. Spence, and K. Kansaku, "Body ownership and agency altered by an electromyographically controlled robotic arm," *Royal Society Open Science*, vol. 5, no. 5, pp. 1–10, May 2018. [Online]. Available: https://royalsocietypublishing.org/doi/10.1098/rsos.172170

[34] M. Slater, "Towards a digital body: The virtual arm illusion," *Frontiers in Human Neuroscience*, vol. 2, 2008. [Online]. Available: http://journal.frontiersin.org/article/10.3389/neuro.09.006.2008/abstract

[35] M. Rohde, M. D. Luca, and M. O. Ernst, "The rubber hand illusion: Feeling of ownership and proprioceptive drift do not go hand in hand," *PLoS ONE*, vol. 6, no. 6. [Online]. Available: https://dx.plos.org/10.1371/journal.pone.0021659

[36] M. Smit, D. I. Kooistra, I. J. M. van der Ham, and H. C. Dijkerman, "Laterality and body ownership: Effect of handedness on experience of the rubber hand illusion," *Laterality: Asymmetries of Body, Brain and Cognition*, vol. 22, no. 6, pp. 703–724, Nov. 2017. [Online]. Available: https://www.tandfonline.com/doi/full/10.1080/1357650X.2016.1273940

[37] M. Rohde, A. Wold, H.-O. Karnath, and M. O. Ernst, "The human touch: Skin temperature during the rubber hand illusion in manual and automated stroking procedures." *PLoS ONE*, vol. 8, no. 11, pp. 1–8, Nov. 2013. [Online]. Available: https://dx.plos.org/10.1371/journal.pone.0080688

[38] M. Gallagher, C. Colzi, and A. Sedda, "Dissociation of proprioceptive drift and feelings of ownership in the somatic rubber hand illusion," *Acta Psychologica*, vol. 212, pp. 1–8, Jan. 2021. [Online]. Available: https://linkinghub.elsevier.com/retrieve/pii/S0001691820305163

[39] S. A. H. Jones, E. K. Cressman, and D. Y. P. Henriques, "Proprioceptive localization of the left and right hands," *Experimental Brain Research*, vol. 204, no. 3, pp. 373–383, Jul. 2010. [Online]. Available: http://link.springer.com/10.1007/s00221-009-2079-8

[40] R. Kondo and M. Sugimot0, "Effects of virtual hands and feet on the onset time and duration of illusory body ownership." *Scientific Reports*, vol. 12, p. 11802, Dec. 2022. [Online]. Available: https://www.nature.com/articles/s41598-022-15835-x

[41] H. H. Ehrsson, B. Rosen, A. Stockselius, C. Ragno, P. Kohler, and G. Lundborg, "Upper limb amputees can be induced to experience a rubber hand as their own," *Brain*, vol. 131, no. 12, pp. 3443–3452, Dec. 2008. [Online]. Available: https://academic.oup.com/brain/article-lookup/doi/10.1093/brain/awn297

[42] A. Kalckert and H. H. Ehrsson, "Moving a rubber hand that feels like your own: A dissociation of ownership and agency," *Frontiers in Human Neuroscience*, vol. 6, no. 40, pp. 1–14, Mar. 2012. [Online]. Available: http://journal.frontiersin.org/article/10.3389/fnhum.2012.00040/abstract

[43] M. Tsakiris, G. Prabhu, and P. Haggard, "Having a body versus moving your body: How agency structures body-ownership," *Consciousness and Cognition*, vol. 15, no. 2, pp. 423–432, Jun. 2006. [Online]. Available: https://linkinghub.elsevier.com/retrieve/pii/S1053810005001200

[44] L. Crucianelli, N. K. Metcalf, A. K. Fotopoulou, and P. M. Jenkinson, "Bodily pleasure matters: velocity of touch modulates body ownership during the rubber hand illusion," *Frontiers in Psychology*, vol. 4, no. 703, pp. 1–7, Oct. 2013. [Online]. Available: http://journal.frontiersin.org/article/10.3389/fpsyg.2013.00703/abstract

[45] S. Bitzer, J. Bruineberg, and S. J. Kiebel, "A bayesian attractor model for perceptual decision making," *PLOS Computational Biology*, vol. 11, no. 8, pp. 1–35, Aug. 2015. [Online]. Available: https://dx.plos.org/10.1371/journal.pcbi.1004442

[46] P. Liashchynskyi and P. Liashchynskyi, "Grid search, random search, genetic algorithm: A big comparison for nas." *arXiv*, pp. 1–11, Dec. 2019. [Online]. Available: http://arxiv.org/abs/1912.06059

Appendices

A Statistics on the experiment

	Estimate	SE	tStat	pValue
(Intercept)	16.718	9.7342	1.7175	0.089407
Group	-1.9482	4.9335	-0.3949	0.69387
Condition	-2.5288	3.3817	-0.74778	0.45659
Time	0.19524	0.089821	2.1737	0.032417

Table 5: **Linear regression model**: $Onsettime \sim 1 + Group + Condition + Time$
Number of observations: 92, Error degrees of freedom: 88
Root mean Squared Error: 14.2
R-squared: 0.0605, Adjusted R-Squared: 0.0285
F-statistics vs. constant model: 1.89, p-value = 0.137

	Estimate	SE	tStat	pValue
(Intercept)	20.541	0.94913	21.642	1.7892e-67
Group	-1.6588	0.51968	-3.1919	0.0015355
Condition	0.80432	0.45115	1.7828	0.075445
Time	0.044844	0.0091512	4.9003	1.4399e-06

Table 6: **Linear regression model**: $Proprioceptivedriftmean \sim 1 + Group + Condition + Time$
Number of observations: 370, Error degrees of freedom: 366
Root mean Squared Error: 4.34
R-squared: 0.0805, Adjusted R-Squared: 0.073
F-statistics vs. constant model: 10.7, p-value = 9.49e-07

	Estimate	SE	tStat	pValue
(Intercept)	2.0564	0.59936	3.431	0.00066993
Group	0.19198	0.32817	0.58501	0.5589
Condition	0.15335	0.2849	0.53827	0.59072
Time	-0.0095753	0.0057789	-1.657	0.098386

Table 7: **Linear regression model**: $Proprioceptivedriftvariance \sim 1 + Group + Condition + Time$
Number of observations: 370, Error degrees of freedom: 366
Root mean Squared Error: 2.74
R-squared: 0.00838, Adjusted R-Squared: 0.0000252
F-statistics vs. constant model: 1.03, p-value = 0.379

	Estimate	SE	tStat	pValue
(Intercept)	-1.6482	0.48937	-3.368	0.00086528
Group	-0.10084	0.26667	-0.37815	0.70561
Condition	1.1492	0.20911	5.4957	8.8762e-08
Time	0.011989	0.0062254	1.9259	0.055149

Table 8: **Linear regression model**: $Ownership \sim 1 + Group + Condition + Time$
Number of observations: 279, Error degrees of freedom: 275
Root mean Squared Error: 1.75
R-squared: 0.11, Adjusted R-Squared: 0.1
F-statistics vs. constant model: 11.3, p-value = 5.05e-07

	Estimate	SE	tStat	pValue
(Intercept)	-2.3046	0.41181	-5.5963	5.2918e-08
Group	-0.085928	0.22441	-0.38291	0.70208
Condition	0.60117	0.17597	3.4163	0.00073062
Time	0.0075395	0.0052388	1.4392	0.15124

Table 9: **Linear regression model**: $Agency \sim 1 + Group + Condition + Time$
Number of observations: 279, Error degrees of freedom: 275
Root mean Squared Error: 1.47
R-squared: 0.0476, Adjusted R-Squared: 0.0372
F-statistics vs. constant model: 4.58, p-value = 0.00379

	Estimate	SE	tStat	pValue
(Intercept)	-0.71167	0.45192	-1.5748	0.11646
Group	-0.65636	0.24627	-2.6653	0.00814879
Condition	0.39802	0.19311	2.0611	0.040232
Time	0.0048308	0.005749	0.84027	0.40148

Table 10: **Linear regression model**: $Control \sim 1 + Group + Condition + Time$
Number of observations: 279 Error degrees of freedom: 275 Root mean Squared Error: 1.61
R-squared: 0.0399, Adjusted R-Squared: 0.0294
F-statistics vs. constant model: 3.81, p-value = 0.0106

B Additional figures

B.1 Scatter plots of the outputs of the onset time, proprioceptive drift and ownership

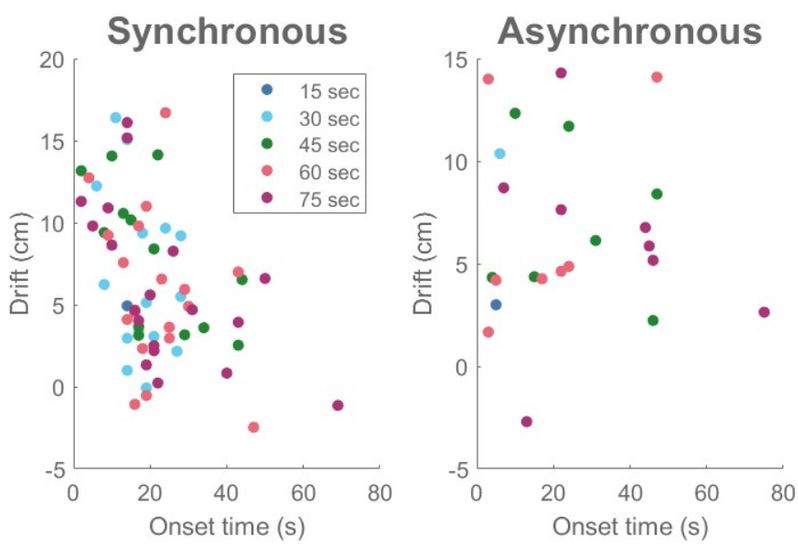

Figure 15: Scatter plot of the given onset time and the corresponding proprioceptive drift for the synchronous and asynchronous condition. The different colors indicate the duration of the stroking.

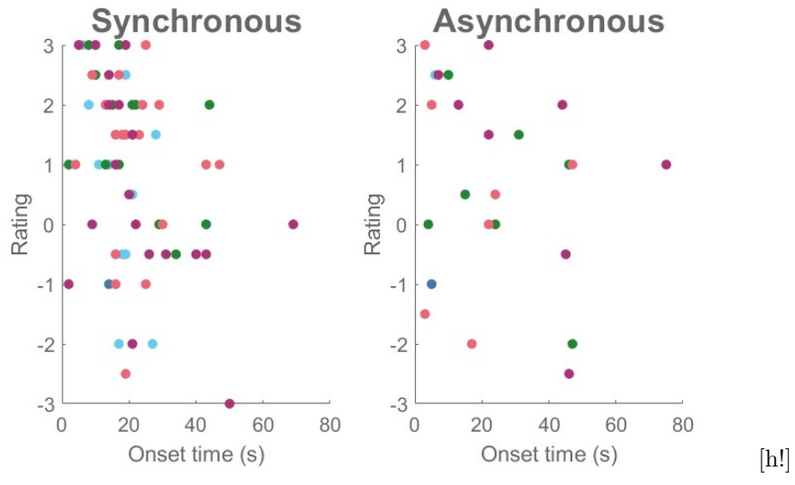

[h!]

Figure 16: Scatter plot of the given onset time and the corresponding ownership statements for the synchronous and asynchronous condition. The different colors indicate the duration of the stroking.

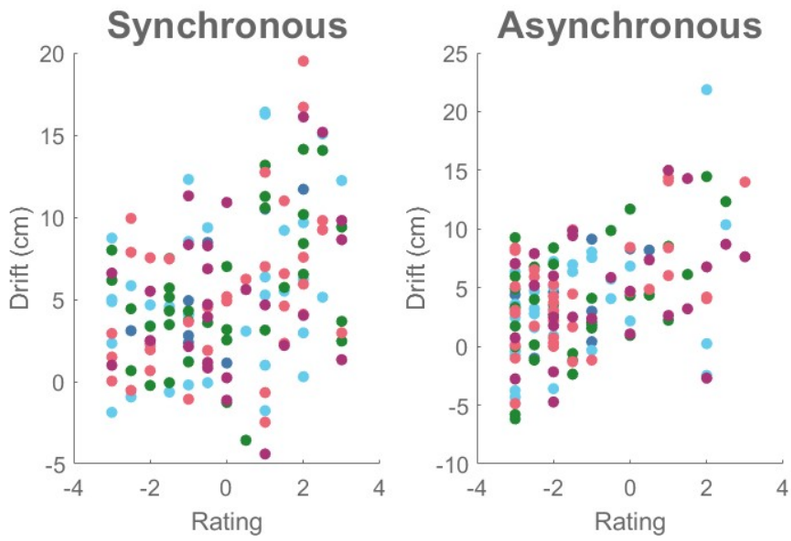

Figure 17: Scatter plot of the given ownership statements and the corresponding proprioceptive drift for the synchronous and asynchronous condition. The different colors indicate the duration of the stroking.

B.2 Figure of the complete dynamical model

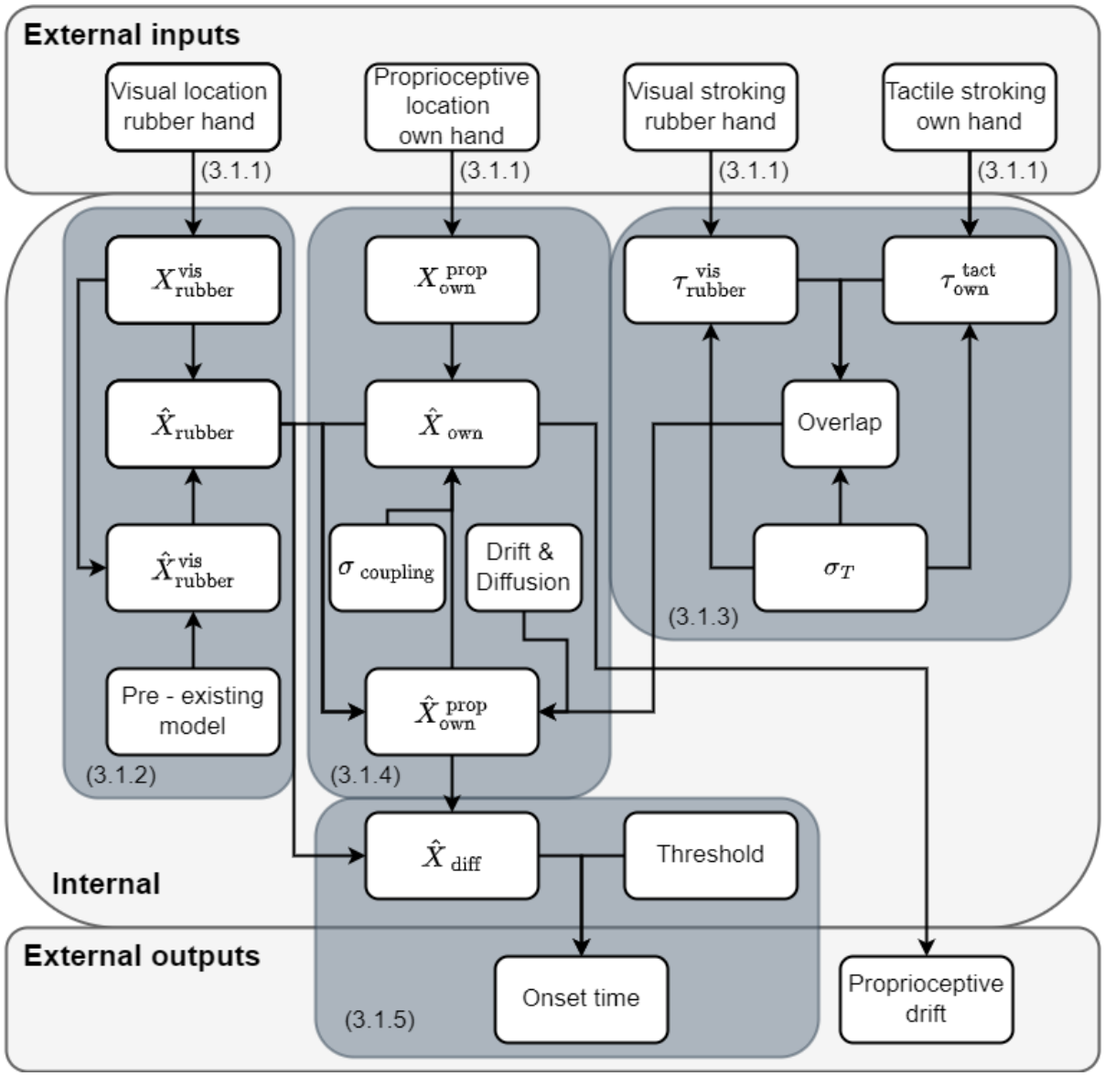

Figure 18: Complete overview of the dynamical model.

C Mathematical explanation of the parameter ranges

C.1 Temporal binding window

Assumption: The stoking is interpreted as synchronous when Overlap > 0.5.

$$\begin{aligned} \text{Area}_{\text{Total}} =& \text{Area}_{\text{seen-stroking}} + \text{Area}_{\text{felt-stroking}} \\ & - \text{Area}_{\text{Overlap}_{\text{seen-over-felt}}} - \text{Area}_{\text{Overlap}_{\text{felt-over-seen}}} \end{aligned} \tag{15}$$

$$\begin{aligned} \sigma_{\text{seen-stroking}} &= \sigma_{\text{felt-stroking}} \\ \text{Area}_{\text{seen-stroking}} &= \text{Area}_{\text{felt-stroking}} \\ \text{Area}_{\text{Overlap}_{\text{seen-over-felt}}} &= \text{Area}_{\text{Overlap}_{\text{felt-over-seen}}} \end{aligned} \tag{16}$$

Integration of equations 15 16 results in equation 17:

$$\text{Area}_{\text{Total}} = 2 * \text{Area}_{\text{seen-stroking}} - 2 * \text{Area}_{\text{Overlap}_{\text{seen-over-felt}}} \tag{17}$$

$$\begin{aligned} \text{Overlap} &= \frac{2 * \text{Area}_{\text{Overlap}_{\text{seen-over-felt}}}}{\text{Area}_{\text{Total}}} \\ \text{Overlap} &= \frac{2 * \text{Area}_{\text{Overlap}_{\text{seen-over-felt}}}}{2 * \text{Area}_{\text{seen-stroking}} - 2 * \text{Area}_{\text{Overlap}_{\text{seen-over-felt}}}} \\ \frac{1}{2} &= \frac{\text{Area}_{\text{Overlap}_{\text{seen-over-felt}}}}{2 * \text{Area}_{\text{seen-stroking}} - 2 * \text{Area}_{\text{Overlap}_{\text{seen-over-felt}}}} \\ 2 * 2 * \text{Area}_{\text{Overlap}_{\text{seen-over-felt}}} &= 2 * \text{Area}_{\text{seen-stroking}} - 2 * \text{Area}_{\text{Overlap}_{\text{seen-over-felt}}} \\ 6 * \text{Area}_{\text{Overlap}_{\text{seen-over-felt}}} &= 2 * \text{Area}_{\text{seen-stroking}} \\ \text{Area}_{\text{Overlap}_{\text{seen-over-felt}}} &= \frac{1}{3} * \text{Area}_{\text{seen-stroking}} \end{aligned} \tag{18}$$

From equation 18 it can be concluded that when the overlap of one of the Gaussian distributions is 33 %, the fraction overlap of the two Gaussian distributions is equal to 0.5 when the delay between the signals and the temporal binding window are equal. To calculate the corresponding variance a z-score of -0.43 and the normal distribution formula:

$$Z = \frac{x - \mu}{\sigma} \tag{19}$$

The intersection of the two Gaussian distributions should be at the center of the two means. Filling in equation 19 with the most extreme values (55-337) results in the variance for both:

$$\begin{aligned} -0.43 = \frac{\frac{55-0}{2} - 55}{\sigma} \quad &\wedge \quad -0.43 = \frac{\frac{337-0}{2} - 337}{\sigma} \\ -0.43 = \frac{27.5 - 55}{\sigma} \quad &\wedge \quad -0.43 = \frac{168.5 - 337}{\sigma} \\ -0.43 = \frac{-27.5}{\sigma} \quad &\wedge \quad -0.43 = \frac{-168.5}{\sigma} \\ -27.5 = -0.43 * \sigma \quad &\wedge \quad -168.55 = -0.43 * \sigma \\ \sigma = 63.95 \quad &\wedge \quad \sigma = 391.86 \\ \sigma^2 = 4090 \quad &\wedge \quad \sigma^2 = 153554 \end{aligned} \tag{20}$$

With these values the linear relationship between the variance and the temporal binding window can be calculated as followed:

$$\begin{aligned} \sigma^2 &= a * \text{temporal binding window} + b \\ 4090 = a * 55 + b \quad &\wedge 153554 = a * 337 + b \\ b = a * 55 - 4090 \quad &\wedge b = a * 337 - 153554 \\ a * 55 - 4090 &= a * 337 - 153554 \\ 282 * a &= 149464 \\ a &= 530 \\ b &= 4090 - 55 * 530 \\ b &= -25061 \\ \sigma^2 &= 530 * \text{temporal binding window} - 25061 \end{aligned} \tag{21}$$

C.2 Coupling prior constant

To let the estimate of the own hand rely solely on external signal, the weighting factor of the external signal must be 1.

$$
\begin{aligned}
\omega_{X_{\text{own}}^{\text{prop}}}(t=0) &= \frac{\sigma^2_{\hat{X}_{\text{own}}^{\text{prop}}}}{\sigma^2_{X_{\text{own}}^{\text{prop}}} + \sigma^2_{\hat{X}_{\text{own}}^{\text{prop}}} + \sigma^2_{\text{coupling}}} \\
1 &= \frac{30}{30 + 15 + \sigma^2_{\text{coupling}}} \\
1 &= \frac{30}{45 + \sigma^2_{\text{coupling}}} \\
30 &= 45 + \sigma^2_{\text{coupling}} \\
\sigma^2_{\text{coupling}} &= -15
\end{aligned}
\tag{22}
$$

Due to the rest of the calculations, the weighting factor will not change over time when a coupling prior constant (C) of -15 is used. This is not the case for the other extreme. To calculate the maximal value of the range, one must look into the formula in which the coupling prior ($\sigma^2_{\text{coupling}}$) is calculated (Equation 8).

To let the estimate of the own hand rely most on the internal signal, the weighting factor of the external signals must be as close to zero as possible. The decay, when a value for the coupling prior greater then 255 is used, is negligible.

From equation 8 follows that more drift between the internal model of the own hand and the estimate of the own hand results in more weighting of the internal signals. With the constraint that maximal drift of the estimate of the own hand is equal to the location of the rubber hand, the maximum value of the coupling prior proprioception can be calculated as followed:

$$
\begin{aligned}
\sigma^2_{\text{coupling}}(t+dt) &= C + \frac{\mu_{\hat{X}_{\text{own}}^{\text{prop}}}(t=0) - \mu_{\hat{X}_{\text{own}}^{\text{own}}}(t)}{\mu_{\hat{X}_{\text{own}}^{\text{prop}}}(t=0) - \mu_{\hat{X}_{\text{rubber}}}(t=0)} * C \\
\sigma^2_{\text{coupling}}(t+dt) &= C + \frac{\mu_{\hat{X}_{\text{own}}^{\text{prop}}}(t=0) - \mu_{\hat{X}_{\text{rubber}}}(t=0)}{\mu_{\hat{X}_{\text{own}}^{\text{prop}}}(t=0) - \mu_{\hat{X}_{\text{rubber}}}(t=0)} * C \\
255 &= C + 1 * C \\
2 * C &= 255 \\
C &= 127.5
\end{aligned}
\tag{23}
$$

D Influence of the internal variables in the dynamical model

For the influence of the parameters, an distance between the hands of 15 cm is used. The delay was set to 500 ms and the duration of the experiment was set to the maximal duration, 600 seconds, with a time interval of 1 second. The initial values of the parameters and the ranges in which the parameters are varied can be found in Table 11

Parameter	**Initial value**	**Ranges**	Figure
Temporal binding window	196	55:1:337	19
Coupling prior constant	56.25	-15:0.5:127.5	20
Drift	0.245	0.01:0.001:0.5	21
Diffusion	0.0245	0.001:0.0001:0.05	22
Height onset threshold	140	0:1:150	23
Decline onset threshold	0.1	0:0.0001:0.2	24

Table 11: The initial values and the ranges in which the influence of the internal variables are visualized

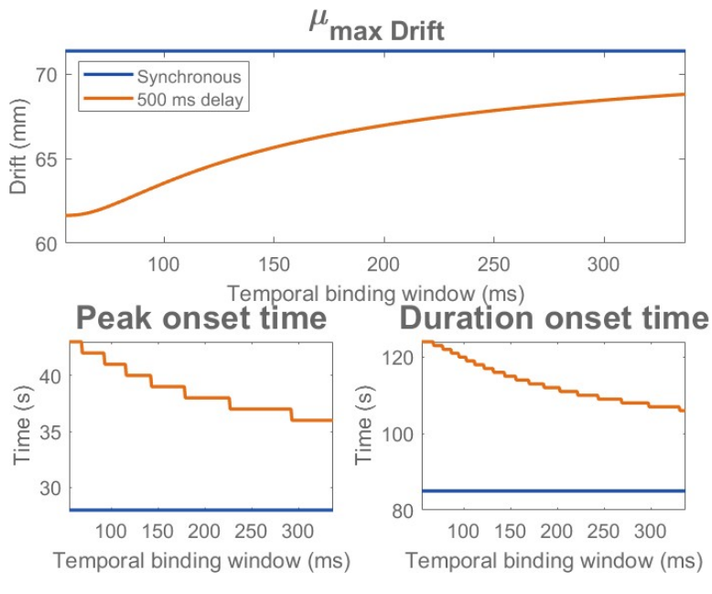

Figure 19: The effects of the temporal binding window

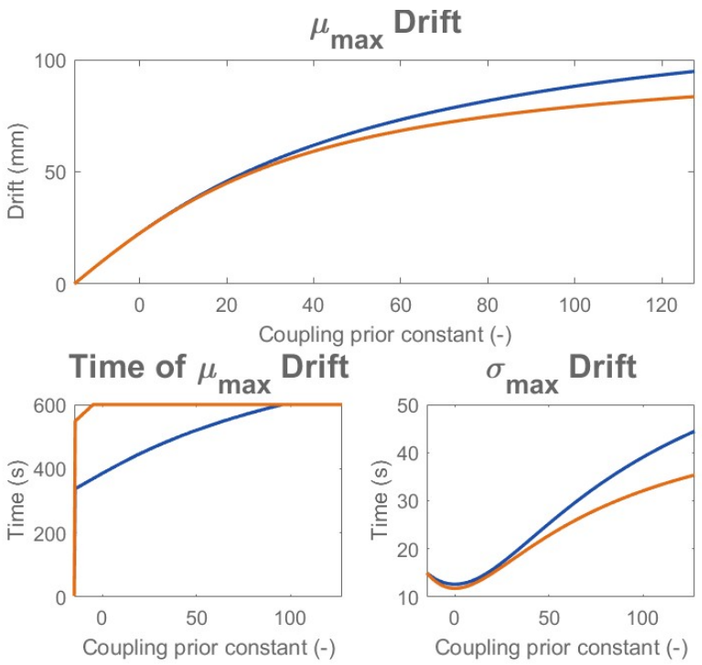

Figure 20: The effects of the coupling prior constant

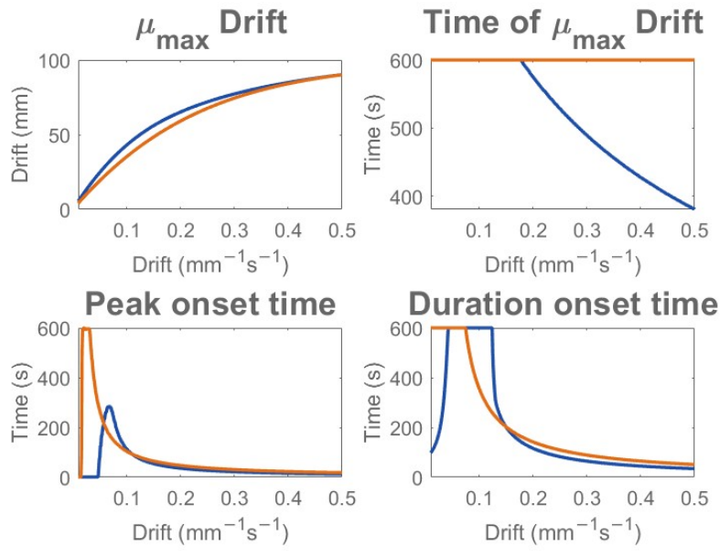

Figure 21: The effects of the drift

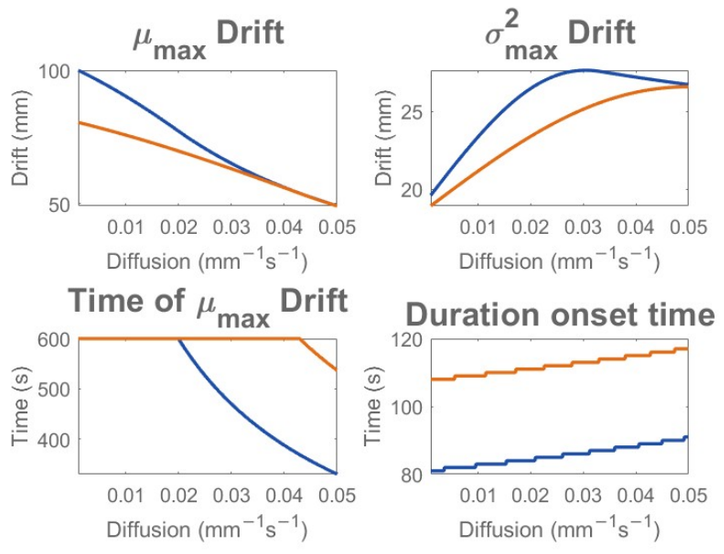

Figure 22: The effects of the diffusion

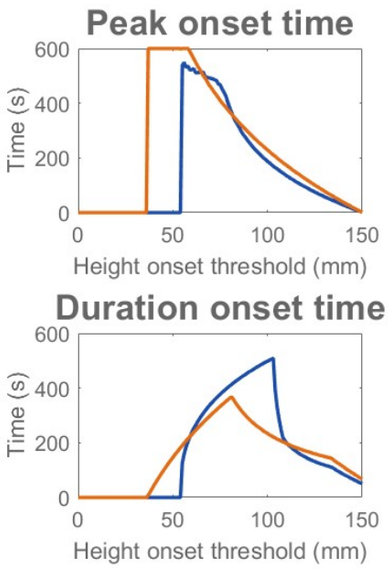

Figure 23: The effects of the height of the onset threshold

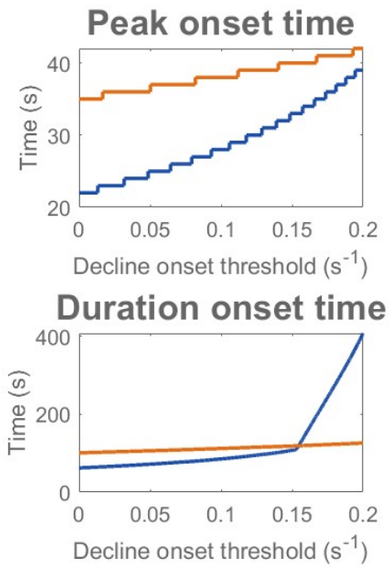

Figure 24: The effects of the decline of the onset threshold